



Expansion and collapse of VEGF diversity in major clades of the animal kingdom

Khushbu Rauniyar¹ · Honey Bokharaie¹ · Michael Jeltsch^{1,2,3,4}

Received: 20 January 2023 / Accepted: 17 March 2023 / Published online: 5 April 2023
© The Author(s) 2023

Abstract

Together with the platelet-derived growth factors (PDGFs), the vascular endothelial growth factors (VEGFs) form the PDGF/VEGF subgroup among cystine knot growth factors. The evolutionary relationships within this subgroup have not been examined thoroughly to date. Here, we comprehensively analyze the PDGF/VEGF growth factors throughout all animal phyla and propose a phylogenetic tree. Vertebrate whole-genome duplications play a role in expanding PDGF/VEGF diversity, but several limited duplications are necessary to account for the temporal pattern of emergence. The phylogenetically oldest PDGF/VEGF-like growth factor likely featured a C-terminus with a BR3P signature, a hallmark of the modern-day lymphangiogenic growth factors VEGF-C and VEGF-D. Some younger VEGF genes, such as *VEGFB* and *PGF*, appeared completely absent in important vertebrate clades such as birds and amphibia, respectively. In contrast, individual PDGF/VEGF gene duplications frequently occurred in fish on top of the known fish-specific whole-genome duplications. The lack of precise counterparts for human genes poses limitations but also offers opportunities for research using organisms that diverge considerably from humans.

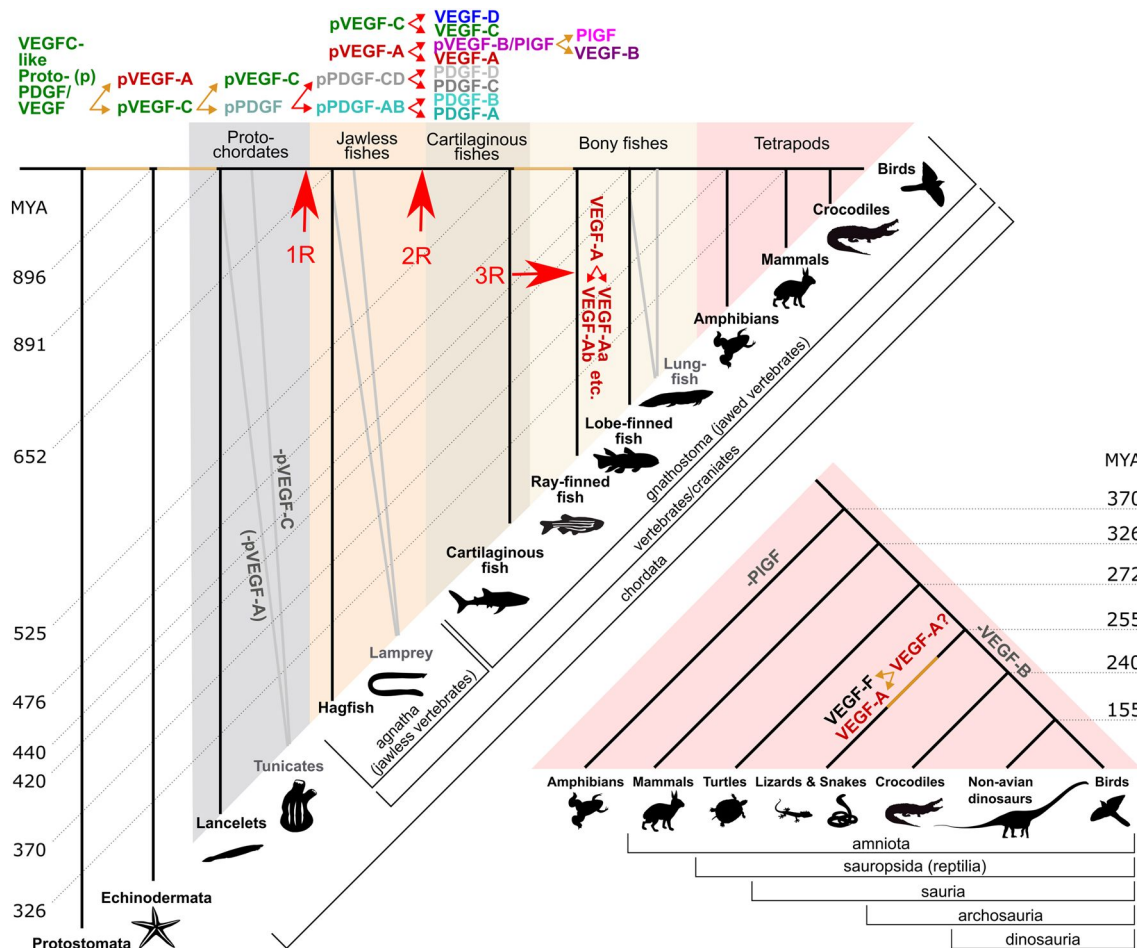
Jeltsch: Phylogeny of the VEGF growth factor family.

✉ Michael Jeltsch
michael@jeltsch.org

- ¹ Drug Research Program, Division of Pharmaceutical Biosciences, Faculty of Pharmacy, University of Helsinki, Biocenter 2, (Viikinkaari 5E), P.O. Box. 56, 00790 Helsinki, Finland
- ² Individualized Drug Therapy Research Program, Faculty of Medicine, University of Helsinki, Helsinki, Finland
- ³ Wihuri Research Institute, Helsinki, Finland
- ⁴ Helsinki One Health, University of Helsinki, Helsinki, Finland

Graphical abstract

Sources for the graphical abstract: 326 MYA and older [1]; 72–240 MYA [2]; 235–65 MYA [3]



Keywords VEGF · PDGF · Phylogeny · VEGF-C · Vascular biology · Evolution

Introduction

In biomedical research, model organisms are often used with the ultimate goal of understanding the human organism. While the mouse is the most common model organism, other species can have specific advantages. Compared to the mouse, *Drosophila melanogaster* has, for example, a much shorter generation cycle, and in zebrafish or chickens, embryonic development can be directly and continuously visually observed.

Extrapolating molecular biomedical research results from a given model organism to humans is facilitated when the human proteins of interest have a corresponding counterpart (ortholog) in the model organism. Therefore, the choice of the mouse as the most common model organism for biomedical research is understandable since, for many protein families, there is a 1:1 relationship of genes and proteins between

Mus musculus and *Homo sapiens*. While there are stunning exceptions (e.g., among the kallikrein-like peptidases) [4], an early estimate found that less than 2% of mouse genes did not have a human counterpart [5]. We were interested in whether this assumption of a 1:1 relationship holds true for the vascular endothelial growth factor (VEGF) family between humans and frequently used model organisms.

The VEGF protein family

The VEGF protein family is a highly conserved subgroup within the cystine knot superfamily of growth factors, which share a conserved cystine knot structure, where six conserved cysteine residues are linked by three disulfide bridges such that two bridges form a ring through which the third bridge passes [6]. In vertebrates, the VEGFs are primarily

involved in angiogenesis and lymphangiogenesis, the two basic mechanisms of how blood and lymphatic vessels grow [7, 8]. The VEGFs signal via the VEGF receptors (VEGFR-1, VEGFR-2, and VEGFR-3), which form a subgroup among the receptor tyrosine kinases (RTKs) that is characterized by seven extracellular Ig-like domains and an intracellular, split kinase domain [9]. Of all VEGFs, VEGF-A was discovered first and soon shown to be of paramount importance for the development of blood vessels as it was the first-ever gene for which a heterozygous deletion was found to be embryonically lethal [10, 11]. Unlike VEGF-A, even the complete loss of the subsequently discovered placenta growth factor (PlGF) and VEGF-B was reasonably well tolerated in mice [12–14]. Thus, VEGF-A has been regarded as the primary, most important VEGF. VEGF-C and VEGF-D, first described in 1996, form a distinct subset within the VEGF family due to their unique structure and function [15, 16]. They feature long, distinct N- and C-terminal propeptides, require multiple proteolytic cleavages for activation, and interact with VEGFR-3, which results in their exclusive ability to directly stimulate the growth of lymphatic vessels in vivo [17–19].

VEGF-E and VEGF-F

Two further VEGF family members have been described: VEGF-E and VEGF-F. VEGF-E is the collective name for VEGF-like molecules encoded by viruses [20], and VEGF-F denotes a group of VEGF-like molecules identified from the venom of snakes, starting with the asp viper in 1990 [21, 22]. In the following years, many venomous snakes were shown to feature similar VEGF-like molecules [23].

VEGF-E sequences are encoded in the genomes of parapoxviruses, and their existence has been tentatively explained by a single horizontal host-to-virus gene transfer event [24], similar to how the oncogenic v-sis (a homolog of PDGF-B) is thought to have been acquired from its simian host [25].

Invertebrate VEGFs

In invertebrates, PDGF/VEGF-like molecules have been identified, many of which are referred to as PDGF/VEGF-like growth factors (PVFs) because their exact relationship to the VEGF and PDGF growth factors appeared unclear. Together, the VEGFs and PDGFs form the PDGF/VEGF superfamily. Likely, PDGFs appeared first in the chordate lineage after the divergence from echinoderms [26, 27]. Correspondingly, their cognate receptors split before the chordates/tunicates divergence into class III and class V RTKs [28]. The fundamental biological change associated with this evolutionary period was the pressurization of the vascular system, and PDGFs are central players in the stabilization

of vessels via mural and smooth muscle cells [29]. Although many PVFs can be identified from invertebrate genomic sequences, only a few have been subjected to functional analysis, including the *D. melanogaster* PVFs and *C. elegans* PVF-1. In vertebrates, VEGF receptors are expressed by cells of vascular endothelial and hematopoietic lineages, and the molecular integration of the immune and the vascular systems appears to be also conserved in invertebrates [30]. A molecular manifestation of this integration is the essential expression of the VEGF receptor-2 (VEGFR-2) by the precursor(s) of both hematopoietic and vascular endothelial lineages [31]. Unsurprisingly, the VEGFR-2 ligand VEGF-C has been shown to be important for various steps in hematopoiesis [32–34].

Opposed to this, no coherent image of the role of PVF signaling in invertebrates has emerged so far. Three separate studies involve *D. melanogaster* PVFs in immune function [35], survival of glia and neural progenitor cells [36], and mobilization of storage fat from adipocytes [37], while the *C. elegans* PVF-1 [38] functions reportedly as a repressor of Netrin signaling in the patterning of the sensillae of the male tail [39].

Five studies describe the phylogenetic relationships within the VEGF family of growth factors [26, 40–43]. However, the studies by Holmes/Zachary and Kasap suffer from a lack of comprehensive data, which were not available in 2005, while the results by Dormer and Beck and He are difficult to parse as they lack sufficient biological context. Thus, we performed a comprehensive analysis of the occurrence of PDGF- and VEGF-like sequences in the animal kingdom and propose, based on our phylogenetic analyses, a likely evolutionary pathway, integrating it with the biological function of the PDGF/VEGF family members.

Results

Coverage

49,992 hits were generated using 676 individual blast searches for homologs of PDGF/VEGF family members. The searches were generated by combining 13 query sequences with 52 animal clades (see Supplementary file1, Fig. S1 for the bioinformatics workflow). 8666 of the blast hits were unique. 90.5% of these hits could be programmatically classified as members of the PDGF/VEGF protein family based on explicit manual annotation of the sequence or the PDGF motif (<https://www.ncbi.nlm.nih.gov/Structure/cdd/cddsrv.cgi?uid=cd00135>). The remaining 9.5% were manually examined and classified. The majority of programmatically unclassified hits appeared to be homologs of the Balbiani ring-3 protein (BR3P), to which the C-terminal domain of VEGF-C bears a striking homology [15]. A very

small number of partial sequences were too short to allow classification, in which case they were excluded from further analysis. A summary of the results is shown in Fig. 1, and a complete table of all hits is shown as Supplementary Table 1, and an interactive online version of the table is available at <https://mjlab.fi/phylo>.

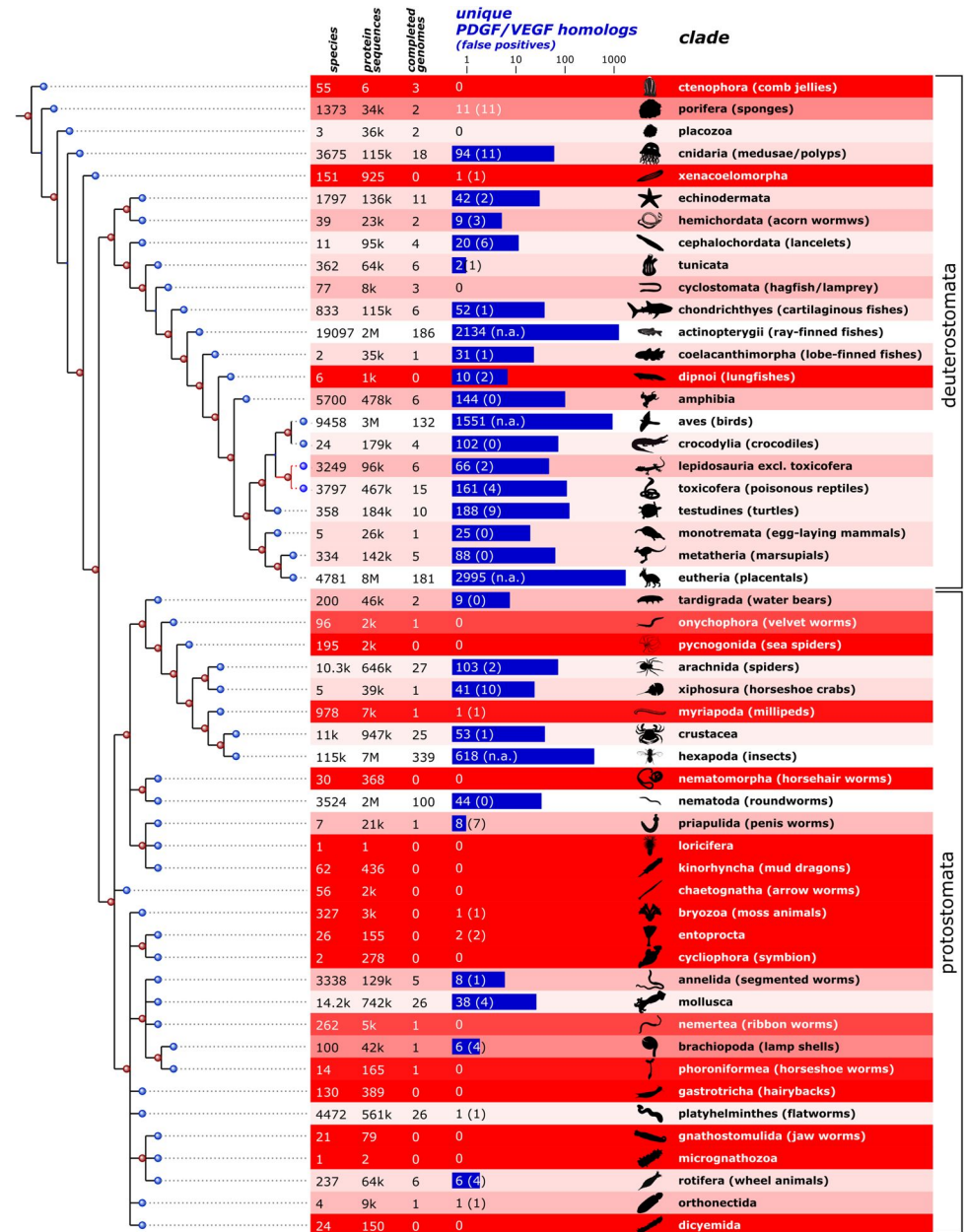
Not all 52 animal clades were equally well represented in the available sequence databases. In underrepresented clades, the absence of evidence for PDGF/VEGF-like genes was not taken as evidence of absence. To visualize this uncertainty, we used a heuristic formula to indicate the bias in the sampling, which takes into consideration the number of animal species of that clade in the NCBI taxonomy

database, the number of sequenced genomes, and the total number of protein sequences for the clade available from the NCBI databases.

PDGF/VEGF-like proteins of the least complex organisms resemble VEGF-C

The least complex animals where PDGF/VEGF-like proteins were identified are the Cnidaria (which include mostly medusae and corals). While 11 blast hits were from Porifera (sponges), which are less complex compared to Cnidaria, all of these were manually identified as false positives (five of these were genuine BR3P or BR3P-like proteins, see

Fig. 1 PDGF/VEGF-like blast hits from 52 animal clades and their quantitative representation in the NCBI taxonomy and sequence databases. The number of blast hits from each clade is indicated in blue. The number of false positive hits is indicated in parentheses. When clades were represented by > 500 species, false positives were not manually excluded (n.a.). The darker the red color, the less reliable the analysis results are due to the underrepresentation of the clade in the sequence databases. Most protostome phyla were underrepresented in the NCBI sequence databases. The current consensus tree of life [44] is shown on the left, aligned with the clades. Note that the relationship of Lepidodosauria to Toxicofera, which might or might not be a clade, is shown with red lines



Supplementary Table 2). From the approximately 115,000 cnidarian protein sequences, 72 were identified as VEGF-like, including the previously described “VEGF” from the marine jellyfish *Podocoryne carnea* and freshwater polyp *Hydra vulgaris* [45–47]. When we analyzed their amino acid sequences and compared them to modern-day VEGFs, they appeared more similar to the modern VEGF-C than to VEGF-A, -B, or PlGF. Similar to VEGF-C and VEGF-D, all but one of these contained the characteristic BR3P motif repeats C-terminally to the VEGF homology domain (VHD) (see Fig. 2). Cnidarian VEGFs typically feature four BRP3 motif repeats after the VHD. Like *Drosophila melanogaster* PVF-2 and *C. elegans* PVF-1, they frequently lack one or both of the cysteine residues which form the intermolecular disulfide bonds in the mammalian PDGFs/VEGFs. When vertebrate PDGF/VEGF homologs are included in the generation of a phylogenetic tree, they cluster into one branch, indicating that PVFs likely originate from a single

VEGF precursor gene in the genome of the most recent common ancestor of Vertebrata and Cnidaria (Fig. 3). In seven out of the 18 gene-annotated Cnidaria genomes, VEGF-like sequences could be identified (*Acropora digitifera*, *Exaiptasia pallida*, *Hydra vulgaris*, *Nematostella vectensis*, *Orbicella faveolata*, *Pocillopora damicornis*, and *Stylophora pistillata*).

Distribution of different VEGFs in the deuterostome branch

We did find VEGF-A-like proteins in Echinodermata, Cephalochordata, and Tunicata, all of which are clades in the deuterostome branch of the animal kingdom. However, all these animals—with the exception of the Tunicata—also contained VEGF-C-like proteins. Among all tunicate sequences, including the six completed tunicate genomes, only one PDGF/VEGF-like gene could be identified. The

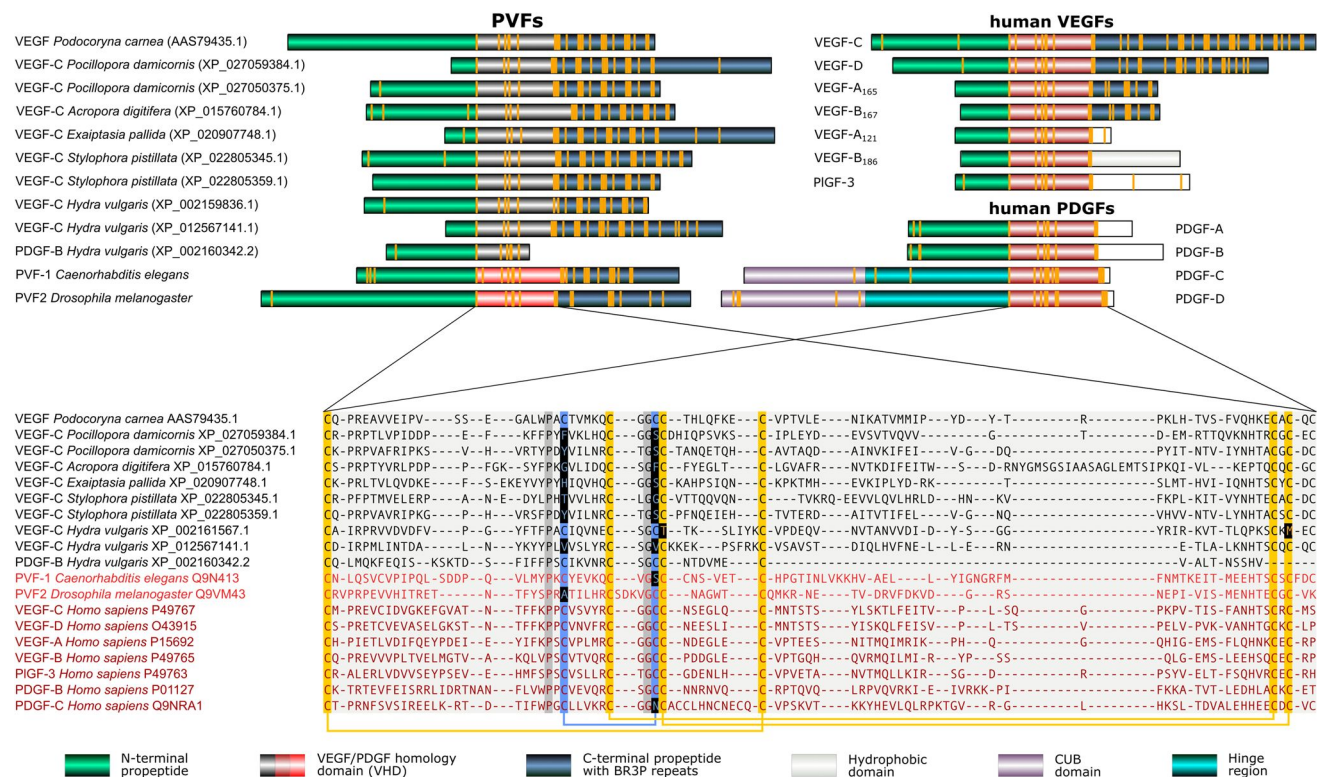


Fig. 2 Comparison of the domain structure and alignment of the VEGF homology domain of cnidarian VEGFs and human PDGFs/VEGFs. Ten representative cnidarian VEGFs (sequences in black) were aligned with human VEGFs, selected PDGFs, *D. melanogaster* PVF-2, and *C. elegans* PVF-1. Most cnidarian VEGFs show a typical cystine knot followed by three to five BR3P motifs similar to the human VEGF-C/D. BR3P motifs are completely absent from mammalian PDGFs and PlGFs, while the longer VEGF-A isoforms and the VEGF-B₁₆₇ isoform contain one complete (CX₁₀CXCXC) and one incomplete (CX₁₀CXC) BR3P repeat C-terminally to the VEGF

homology domain. In the alignment, the cysteines of the cystine knot are shown on an orange background, and the cysteines forming the intermolecular disulfide bridges are on blue background. The intermolecular disulfide bridges frequently appear absent in invertebrate VEGFs (marked by inverted coloring), but some of this might be an artifact of the alignment. 100% conserved non-cysteine residues are shown on dark gray background. The bridging pattern of the canonical PDGF/VEGF cysteines is indicated by connecting lines below the alignment

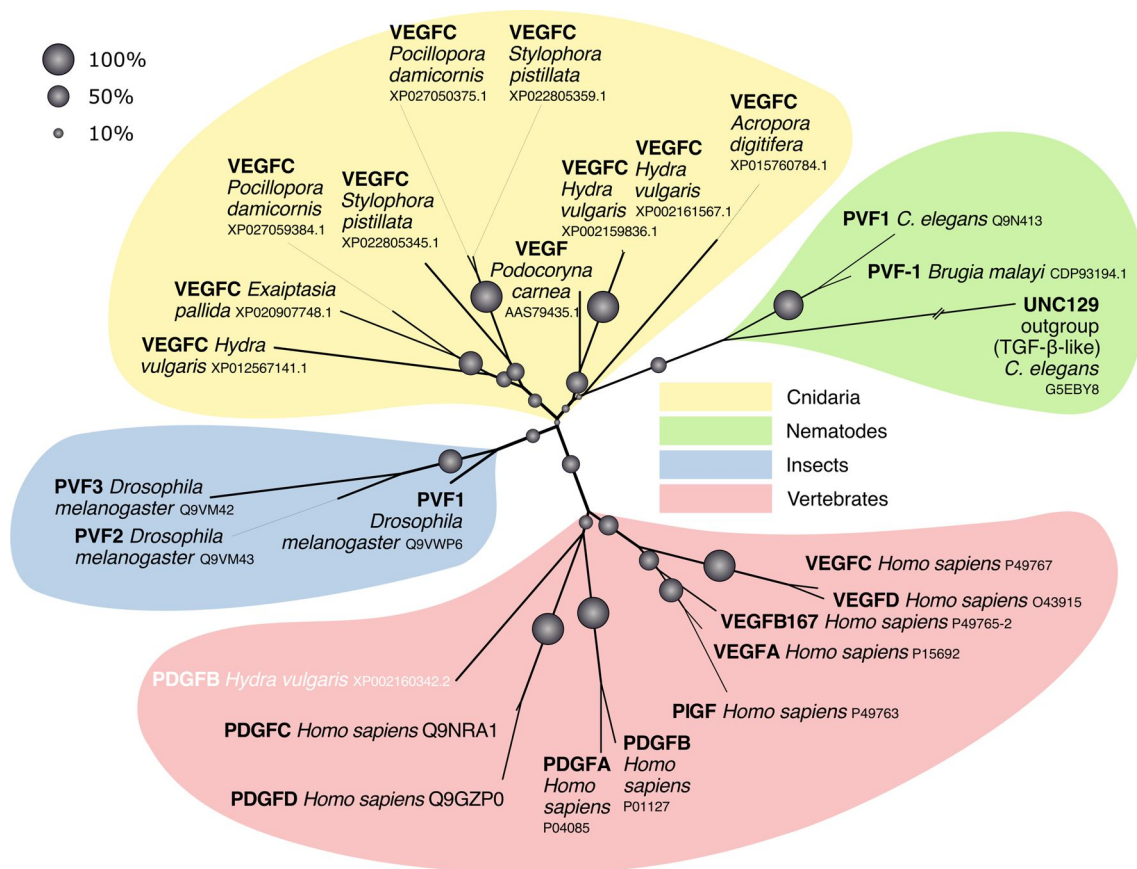


Fig. 3 Vertebrate versus invertebrate VEGFs. A phylogenetic tree was calculated from an expanded set of sequences, aligning mostly the PDGF/VEGF homology domains. In this unrooted tree, *Podocoryna carnea* VEGF groups clearly together with all the other cnidarian VEGF-C-like sequences, the exception being *Hydra vulgaris* PDGF-B (shown in white font color), which consistently groups

with the mammalian PDGF-C/D group, with which it also shares other characteristics such as the near-complete lack of C-terminal sequences beyond the PDGF/VEGF homology domain. The confidence into branches is given as bootstrap values (% from 1000 repeats)

amino acid sequence of the predicted corresponding tunicate gene product showed a close homology to VEGF-A.

Not being a formal taxonomic group, there is considerable heterogeneity among fish. In bony fish (Osteichthyes), all five mammalian VEGFs (VEGF-A, PIGF, VEGF-B, VEGF-C, and VEGF-D) are ubiquitous. Previously, cartilaginous fish (Chondrichthyes: sharks, rays, skates, sawfish, and chimeras) were thought to lack PIGF and VEGF-B, but we could find, in the majority of species, sequences that showed the closest homology to PIGF and VEGF-B, respectively (Supplementary file1, Fig. S2). Only jawless fish (Cyclostomata: lamprey and hagfish) seem to be devoid of orthologs for PIGF, VEGF-B, and VEGF-D. When plotted along the branches of the phylogenetic tree of the animal kingdom, there is an overall expansion of VEGF diversity over time, while a few major branches undergo a collapse (Fig. 4). The collapse coincides with a reduction in body plan complexity in the case of the Tunicata, which have either reduced the number of VEGF paralogs by eliminating VEGF-C-like

sequences (*Ciona intestinalis*) or functional VEGF genes altogether (all other tunicates analyzed). However, a similar reduction of body plan complexity is not seen for the clade Archosauria with its extant members (birds and crocodiles), in which we did not find any signs of functional *VEGF-B* genes. The same holds for Amphibia, in which we did not find functional genes coding for Placenta growth factor (Pgf). While we also did not detect any VEGF-B in Monotremata or any PDGF/VEGF-like proteins in Xenacoelomorpha, we did not consider these findings significant due to the incomplete sampling of these phyla in the sequence databases.

Whole-genome duplications only partially explain the expansion of the PDGF/VEGF family

Whole-genome duplications (WGD) have contributed significantly to the increasing complexity of gene families and vertebrate evolution [48, 49]. When we overlaid the

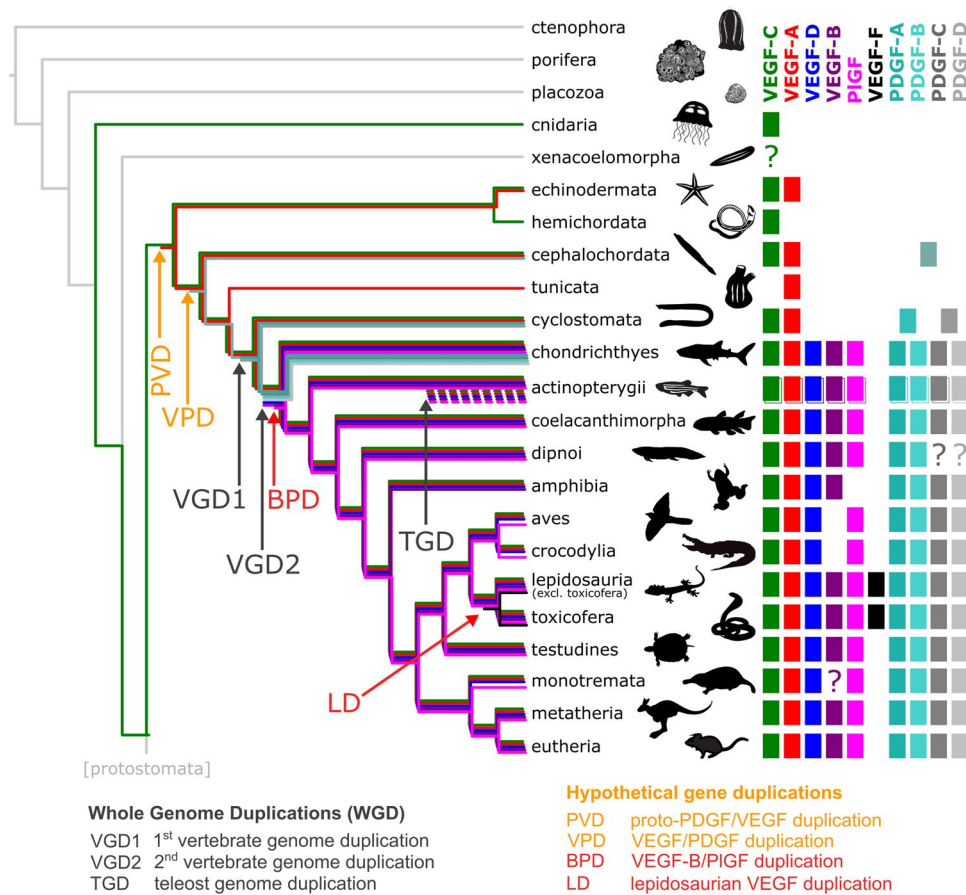


Fig. 4 Occurrence of PDGF/VEGF genes in genomes of extant animal clades (excluding protostomes). Inferring from the occurrence of PDGFs/VEGFs in extant animal species, the first PDGF/VEGF-like protein appeared before the deuterostome/protostome split (DPS) and was likely most similar to the modern VEGF-C. The earliest expansion (proto-PDGF/VEGF duplication, PVD) appears after the DPS but prior to the known first vertebrate genome duplication (VGD1). One of the duplicated proto-PDGFs/VEGFs underwent partial removal of its C-terminal domain, resulting in a VEGF-A-like protein. The subsequent expansion of the family likely results from VGD1 and VGD2. Many mammalian genes have two orthologs in zebrafish that result from teleost genome duplication (TGD). Separate, limited gene duplication events (red arrows) explain the emergence of PIGF and VEGF-B soon after the VGD2 duplication (VEGF-B/PIGF duplication, BPD) and, more recently, of VEGF-F (Lepidosauria duplication, LD). Due to gene loss, some clades appear

devoid of all or some VEGFs (VEGF-C: Tunicata, PIGF: Amphibia, VEGF-B: Aves, Crocodylia). In tunicates, the gene loss concurs with a massive reduction in morphological complexity, but not in amphibians, birds, and crocodiles. The separation of VEGFs and PDGFs (VEGF/PDGF duplication, VPD) likely happened soon after the first duplication of the proto-PDGF/VEGF as already Cephalochordata feature a single PDGF-like gene (see Supplementary file1, Fig. S2). Note that the absence of all VEGFs in Xenacoelomorpha, VEGF-B in Monotremata, and PDGF-C/D in Dipnoi could be due to the underrepresentation of these clades in the available sequence data. For reasons of clarity, the figure does not show **a** the PDGFs lines on the branch leading to mammals starting from the VGD2 (since they are consistently present on that branch), **b** the salmonid genome duplication (SaGD), **c** individual gene duplications not found in the majority of species of the tree branch (such as VEGF-C and PDGF-A duplications in some sharks and other fishes)

established WGDs and the emergence of novel PDGF/VEGF paralogs on the phylogenetic tree of the animal kingdom (Fig. 4), the emergence of novel PDGF/VEGF family members coincides only partially with the proposed timing of the three WGDs. The first PDGF/VEGF (“Proto-PDGF/VEGF”) appears in the tree before the deuterostome/protostome split (DPS), but diversification is likely to have happened only after the DPS since the protostome branch lacks the diversification pattern seen in the deuterostome branch. In the deuterostome branch, the first diversification happened

likely at the protochordate stage, prior to the first vertebrate whole-genome duplication (VGD1). PVFs from species in the protostome branch of the tree (insects, nematodes) do not show a clear diversification into distinct subgroups as seen in the vertebrate lineage, where PDGFs, angiogenic VEGFs (VEGF-A, -B, and PIGF), and lymphangiogenic VEGFs (VEGF-C and -D) have formed distinct subgroups. Already species that diverged soon after the DPS (Echinodermata) feature two distinct VEGF homologs, which resemble the shorter, angiogenic VEGFs (VEGF-A-like) and longer,

lymphangiogenic VEGFs (VEGF-C-like), followed soon by the separation of the PDGF branch, which becomes established before the divergence of the cephalochordate branch.

The VGD1 and VGD2 occurred within the direct line to mammals, while the third significant WGD event took place in the common ancestor of the teleost fish lineage [50], to which also zebrafish (*Danio rerio*) belongs. Although the VGD1 must have resulted in a duplication of the *proto-VEGF-A* and *proto-VEGF-C* genes, resulting in four VEGF homologs, we did not find any evidence that any of the duplicated *VEGF* genes permanently became established in the genome. Different from this, VGD1 is likely to have established the two PDGF subgroups by duplicating the *proto-PDGF* gene. However, a clear separation into a PDGF and a VEGF lineage had not occurred at this stage (see Supplementary file1, Fig. S2), and the proposed order of events is, therefore, the most parsimonious but not the only possible.

The VGD2 likely gave rise to the VEGF-C/VEGF-D subfamily by duplication of the *proto-VEGF-C* gene, and to the VEGF-A/PIGF/VEGF-B subfamily by duplication of the *proto-VEGF-A* gene. The emergence of the third member of the VEGF-A/PIGF/VEGF-B subfamily shortly after

VGD2 and the emergence of VEGF-F are most parsimoniously explained by limited duplications in the common ancestor of all Actinopterygii and the common ancestor of all Lepidosauria, respectively.

Duplicated and missing PDGFs/VEGFs

Because of recent discoveries in the developmental pathways of the fish vasculature [51], we wanted to know how successfully PDGF/VEGF ohnologs (WGD-generated homologs) withstood inactivation/pseudogenization and whether PDGF/VEGF gene duplications can also be found in clades outside the teleost lineage. Thus, we analyzed RNAseq data from all fish species present in the FishPhylo database [52] (Fig. 5). Despite significant heterogeneity, ohnologs of PDGFs/VEGFs were identified in most other fishes, with the expected exception of the Holostei (bowfin and spotted gar). A notable exception in the teleost lineage is *vegffb*, for which we did not find a single mRNA contig, and *pdgfa*, which seems to have been lost in five out of six salmonid species. Salmonids, on the other hand, show clear signs of having maintained some of their other PDGF/VEGF

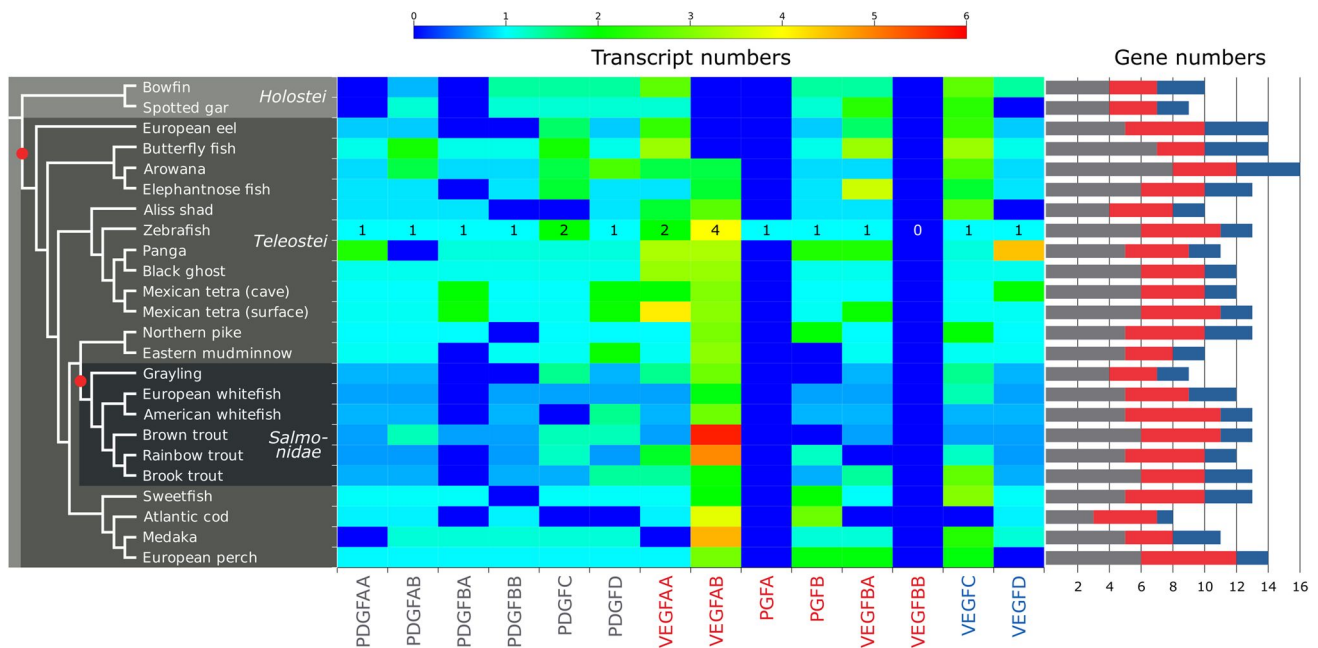


Fig. 5 Numbers of different PDGF/VEGF mRNA transcript contigs and corresponding genes in 24 fish species as determined by RNA sequencing. While Holostei fishes did not undergo the teleost genome duplication (TGD), they nevertheless feature individually duplicated genes such as *vegfc*. After the TGD, salmonids did undergo one additional round of genome duplication (salmonid genome duplication, SaGD) and, consequently, may feature—compared to humans—up to 4 times as many genes for each PDGF/VEGF, resulting theoretically in up to 36 different *pdgf/vegfc* genes. About 20–50% of genes are functionally maintained after whole-genome duplications due to

neo- or subfunctionalization [53–56]; therefore, the expected number of functional *pdgf/vegfc*-like genes in salmonids is between 12 and 20, which is in line with the number of genes deduced from the mRNA transcripts (Supplementary Tables 3 and 4). The heatmap has been normalized to zebrafish mRNA transcript numbers to compensate for the differences in the total number of mRNA transcript contigs obtained for each species. Whole-genome duplications are shown as red dots on the cladogram on the left. Note that the transcript number is only weakly associated with the gene number

ohnologs originating from the salmonid genome duplication (SaGD), most notably VEGF-A ohnologs.

We found VEGF-C duplicated in the fish clade Holostei, which diverged from teleosts before the teleost genome duplication. Only eight extant species comprise the extant Holostei lineage (the bowfin and seven gar species). All three fully sequenced genomes (*Amia calva*, *Atractosteus spatula*, and *Lepisosteus oculatus*) feature a duplicated *vegfc* gene indicating a single gene duplication early in the Holostei lineage (Fig. 6a). When testing whether the *vegfc* genes in these fishes are still under purifying selection (i.e., whether gene inactivation or mutations are detrimental), we detected strong pervasive purifying selection throughout the coding region, with the strongest conservation in the receptor binding domain, followed by the silk homology domain (SHD) (Fig. 6b). Among all fish species, individual gene duplications were found frequently for VEGF-C but occasionally also observed for other genes such as VEGF-A (Fig. 6c).

Our results initially indicated a complete absence of PDGFs/VEGFs in the extant jawless fishes (Cyclostomata) sea lamprey (*Patromyzon marinus*) and inshore hagfish (*Eptatretus burgeri*). We reasoned the lack of cyclostomate PDGF/VEGFs in protein databases to be an artifact, perhaps due to a failure of gene prediction or annotation. A manual inspection of the Ensemble [57] lamprey and hagfish genomes showed—as predicted by our phylogenetic tree—four PDGF/VEGF-like sequences; and an update to the Ensemble genebuild pipeline added the proteins to the Uniprot database in 2022 (see Supplementary file1, Fig. S2). However, the inshore hagfish sequences have not yet been migrated to the (blastable) NCBI protein database.

Having identified PDGF/VEGF-like proteins in seven Cnidaria species, we reasoned that their absence in other cnidarians could also be an artifact. We scrutinized the genomic sequence of *Thelohanellus kitauei* but could not identify genes coding for PDGF/VEGF-like proteins using relaxed degenerate search criteria. *T. kitauei* belongs to the endoparasitic myxozoa branch of Cnidaria, which is characterized by a reduction in genome size and gene depletion [58], explaining the lack of PDGF/VEGFs in parasitic Cnidaria.

Both VGD1 and VGD2 contribute to PDGF expansion

Kipryushina et al. [26] place the emergence of PDGFs after the divergence of Echinoderms and Chordates, notwithstanding early reports of PDGF/PDGFR signaling in sea urchins [59]. Concurring with Kipryushina, the PDGF/VEGF-like proteins identified from the known 11 sea urchin genomes are highly homologous to the proto-VEGF-C that we found in Cnidaria, and we found the first PDGF-like growth factors in Cephalochordata (lancelets). Lancelet genomes feature one or two PDGF-like growth factor genes

and one VEGF-C-like gene (see Supplementary file1, Fig. S2). However, only VEGF-C-like growth factors can confidently be placed into the corresponding ortholog group due to their BR3P signature. Most tree topologies placed the other cephalochordate PDGF/VEGF family members between VEGF-Cs and PDGFs, albeit with low bootstrap support values. The cephalochordate PDGFs/VEGFs were likely duplicated by VGD1 since Cyclostomata (hagfish, lamprey) already feature four PDGF/VEGF genes. While the VGD2 explains the emergence of PDGF-C and PDGF-D by duplicating the proto-PDGF-C/D, the exact order of the preceding events in the early VEGF/PDGF evolution cannot be reconstructed with confidence as the support values of the phylogenetic tree reconstructions remained low, independently of the methods used (see Supplementary file1, Fig. S2). This is not surprising if assuming a monophyletic origin of Cyclostomata [60, 61] but results in the fact that the sequences from Cyclostomata are not very informative about the early PDGF/VEGF evolution.

VEGF-F can be found in several Lepidosauria, not only in venomous snakes

In 1999, it was recognized that the hypotensive factor from the venom of *Vipera aspis* [21] is a VEGF-like molecule [22]. Our analysis shows that VEGF-F is not limited to venomous snakes but is also found in non-venomous snakes (e.g., *Python bivittatus*, XP_025024072.1) and lizards, independently of whether they are venomous or not (see Supplementary file1, Fig. S3). Amino acid sequence alignments of VEGF-Fs show a similar high homology to both VEGF-A and PIGF, and based on phylogenetic trees, it appears likely that either VEGF-A or PIGF served as an evolutionary template for VEGF-F. Because we identified VEGF-F orthologs also in lizards, e.g., in the common wall lizard (*Podarcis muralis*, XP_028597744.1) or the gekko (*Gekko japonicus*, XP_015284783.1), the gene duplication likely happened early in the Lepidosauria lineage, before the invention of venom. However, we found a clear subdivision in the VEGF-F branch between “viper” VEGF-Fs and “non-viper” VEGF-Fs. Only for the VEGF-Fs from the viper branch the venom character of the VEGF-Fs has been experimentally verified.

Viral VEGFs

Another biological entity that has co-opted PDGFs and VEGFs for its own purposes is viruses. To analyze the relationship between all available viral VEGF sequences (VEGF-Es), we constructed a phylogenetic tree of all VEGF-E sequences that were identified in the main analysis (see Fig. 7 for the simplified tree and Supplementary file1, Fig. S4 for the complete tree). Sequences coding for VEGF-like genes were found in the genomes of at

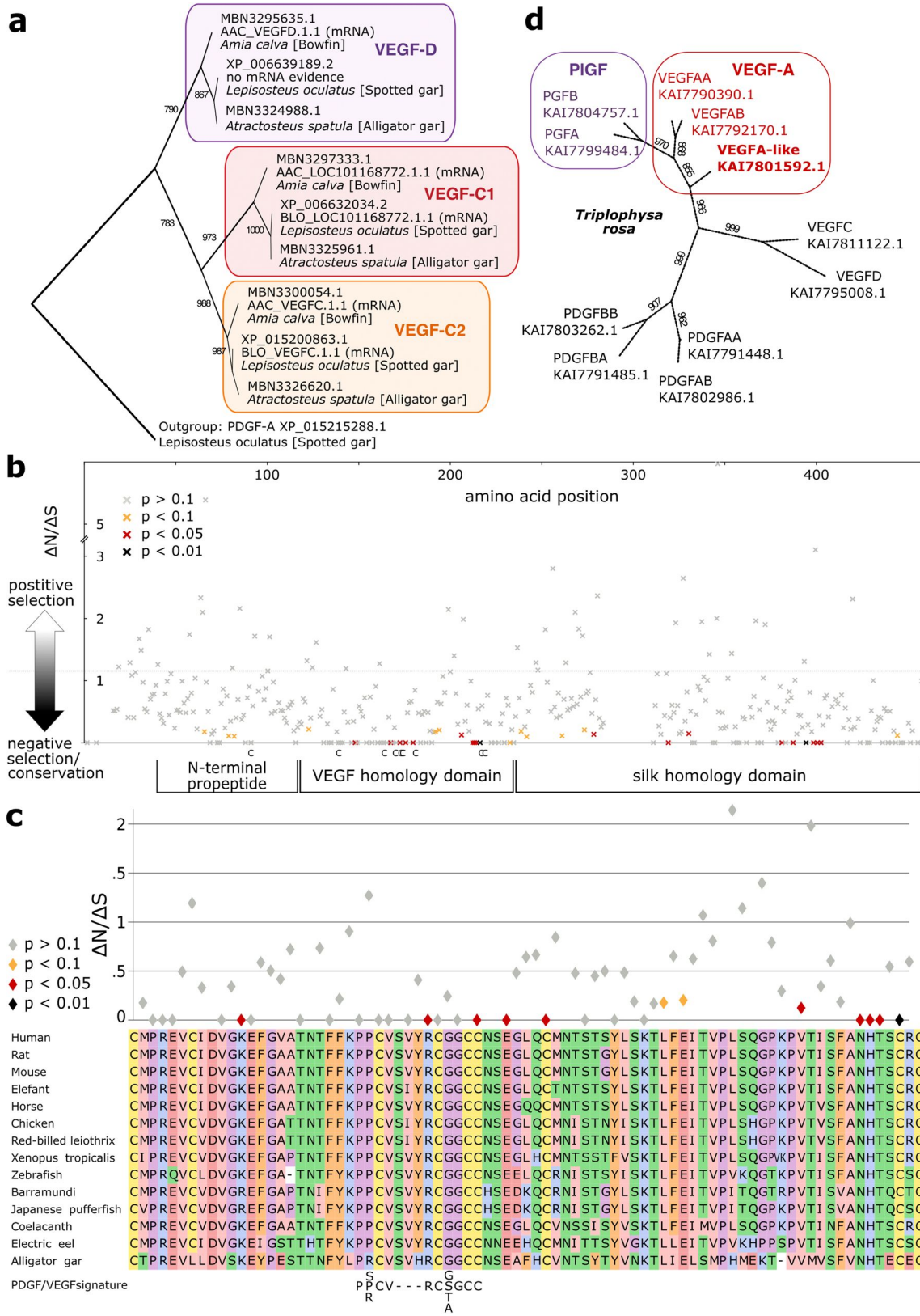


Fig. 6 Individual gene duplications contribute to VEGF diversity in fishes. **a** The *vegfc* gene is duplicated in all Holostei species, and for the bowfin and the spotted gar, there is mRNA evidence for gene expression of both paralogs, while there was no evidence for the expression of *vegfd* in the Spotted gar (see also Supplementary Table 4). **b** Holostei *vegfd* and *vegfc* genes are under purifying selection, most notably in the VEGF homology (VHD) and silk homology domain, where there appears to be strong pressure to maintain the cystine knot structure. Cysteine residues of the VHD are indicated below the x-axis. **c** Detailed view on the conservation of the VHD, aligned with representative VEGF-C amino acid sequences and the PDGF/VEGF signature. Please note that sites without synonymous codon changes ($\Delta S=0$) are not displayed. **d** *vegfa* is also sometimes individually duplicated in some fish species, as shown for *Triplophysa rosa*

least four different virus clades: orf virus (ORFV), pseudocowpoxvirus (PCPV), bovine pustular stomatitis virus (BPSV), and megalocytivirus (MCV). ORFV, PCPV, and BPSV are collectively known to infect at least ten mammalian species, while MCVs have been detected in at least eight fish species. The most parsimonious phylogenetic trees suggest that VEGF-Es originate from VEGF-A. We did not find any evidence of recent multiple host-to-virus gene transfers as all vertebrate VEGFs formed tight clusters, which were well separated from the VEGF-E clusters. We did not observe a separation of the host species with the phylogeny. However, only the ORFV cluster probably contains enough sequences to allow for any such separation to become apparent.

PDGF/VEGF-like molecules of the protostome branch

The sequence coverage of the protostome branch of the animal kingdom was much weaker than that of the deuterostome branch. For 16 out of 29 invertebrate phyla, we could not find a single genomic draft sequence, and almost all available genomic data covered only six phyla: flatworms, roundworms (nematodes), mollusks, crustaceans, insects, and spiders. While nematodes and flatworms do not possess blood circulation, insects, spiders, and crustaceans feature a so-called open circulation, where the hemolymph is circulated inside a body cavity (hemocoel). PDGF/VEGF-like molecules were identified in all these six phyla except for flatworms. Less than half of the 100 completed nematode genomes contained PDGF/VEGF-like genes. Among these are notably many *Caenorhabditis* PVFs, like *C. elegans* PVF-1 (NP_497461.1), but the majority were found from parasitic nematodes, including intestinal parasites like *Ancylostoma duodenale* (KIH56282.1), lymphatic parasites like *Brugia malayi* (CDP93194.1) and *Wuchereria bancrofti* (VDM19972), and conjunctival parasites like *Loa loa* (XP_003142823.1). PDGF/VEGF-like proteins appear

common, if not pervasive, among mollusks, crustaceans, insects, and spiders and can be identified in most genome-sequenced species.

Conservation of the VEGF sequences

Except for VEGF-A and VEGF-C, the physiological and pathophysiological role of VEGF family members is still under debate. Some of them (*Vegfb* and *Vegfd*) can be deleted in mice without any major phenotype [12, 13, 63]. To compare the evolutionary pressures acting on different VEGFs, we analyzed the conservation of their coding sequences. We compared nonsynonymous and synonymous substitution rates inferred by a maximum-likelihood approach. The VEGF-C sequence was most strongly conserved, followed by VEGF-D, while PlGF showed the highest variability while still being relatively conserved. VEGF-A was overall also very conserved but showed a peak of variability at the very end of the VHD corresponding to loop 3, which is a major carrier of the receptor binding epitopes for VEGF (Fig. 8).

VEGF-A splice isoforms

Splice isoforms are a means of generating diversity at the protein level from a single gene. Within the PDGF/VEGF family, alternative mRNA splicing is very unequally used to generate diversity: the hemangiogenic VEGFs (VEGF-A, PlGF, and VEGF-B) all feature at least two major splice isoforms, while the lymphangiogenic VEGFs (VEGF-C and VEGF-D) seem to generate all of their protein diversity post-translationally by alternative proteolytic processing [67]. The Uniprot protein entry for human VEGF-A describes no less than 17 splice isoforms, eight of them with evidence at the protein level. When reimplementing the DIVAA software [68] in Biopython to quantify the diversity of VEGF sequences, we realized that for genes rich in splice isoforms such as VEGF-A, an accurate assignment of isoforms is paramount since indels are not handled well by alignment and tree-building algorithms. Using the length of the coding region and comparisons with a reference list of known VEGF-A mRNA isoforms, we programmatically sorted VEGF-A protein sequences into four major buckets, corresponding to the human 121, 165, 189, and 206 isoforms. When we counted the number of sequences for these four VEGF-A isoforms, we found a ratio of roughly 9:4:3:1 for the 189, 165, 121, and 206 isoforms, indicating that VEGF-A₁₈₉ might be the predominant VEGF-A isoform in many species.

We further investigated the potentially antiangiogenic VEGF-A_{XXX}b and VEGF-Ax isoforms, which are generated using an alternative downstream splice acceptor site in exon 8 (VEGF-A_{XXX}b) [69] or read-through translation

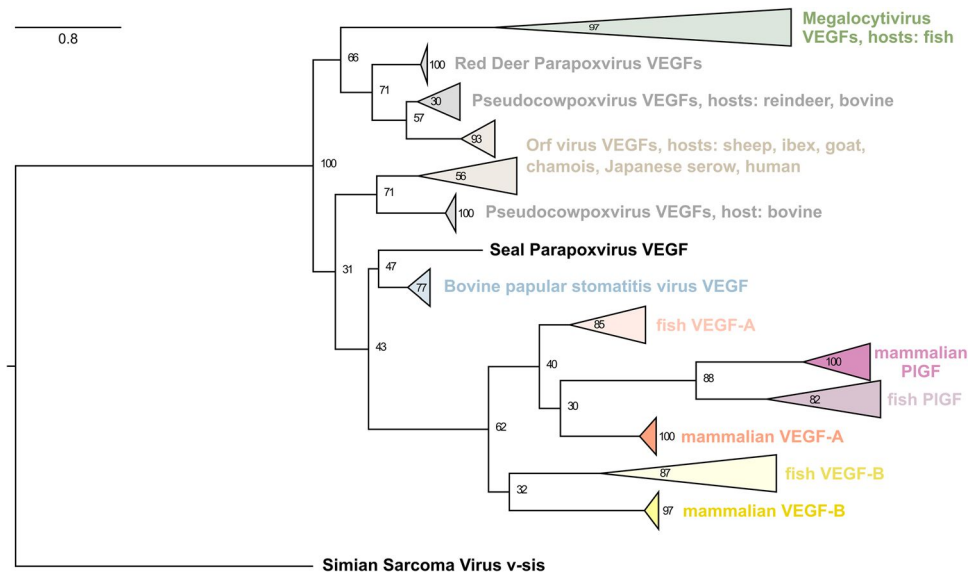


Fig. 7 Phylogenetic protein tree of VEGF-E. Without exception, all VEGF-E and all non-viral VEGF sequences cluster together, arguing that none of the known VEGF-Es originates from recent host-to-virus gene transfer events. The protein tree is compatible with a single origin of all VEGF-E, but due to the significant distance, convergent evolution cannot be excluded. Based on the VEGF sequence alone, assignment to the Pseudocowpoxvirus or Orf virus group is not pos-

sible since several VEGF sequences derived from different viruses are identical (e.g., reindeer PCPV VEGF is identical to the VEGF sequence from the PCPV reference genome VR634). In this branch of the tree, cross-species transmissions have been reported, including to humans [62]. The expanded tree with all leaves is shown in Supplementary file1, Fig. S4

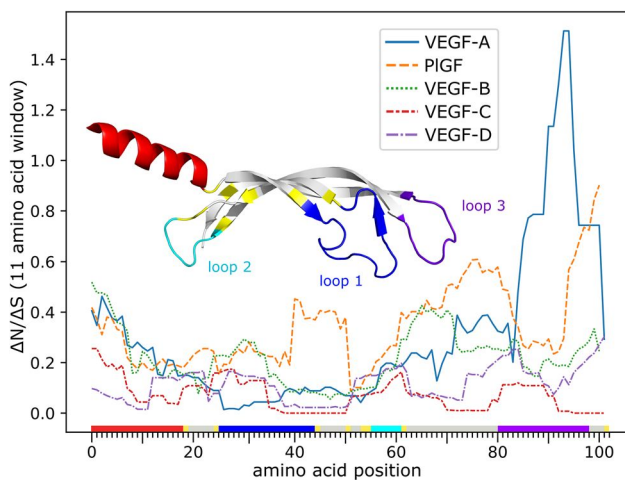


Fig. 8 Conservation of the VEGF homology domain. The ratio of nonsynonymous to synonymous mutations was inferred for all sites over the whole tree and averaged over an 11-amino acid window. VEGF-C shows the highest conservation, while the evolutionary younger family members appear to be more volatile. The amino acid position on the x-axis is color-coded to correspond to the location of the residue in the 3D structure of the monomeric VEGF-C protein [64]. Note that the peak at the end of the VEGF-A sequence might or might not be an artifact resulting from the difficulty of generating a good alignment for loop 3 (shown in purple). Alternatively, the peak might correspond to adaptations in the receptor interaction, as loop3 carries major determinants for receptor binding [65, 66]

of exon 8 (VEGF-A_x) [70]. We found that the possibility to generate these by non-canonical splicing is conserved in mammals but does not generally extend to other animal classes. Comparing nonsynonymous with synonymous substitution rates in the coding sequences of exon 8 and 9, we found evidence of purifying selection at two of the six sites in exon 8 (VEGF-A), one site in exon 9 (VEGF-A_{xxx}b), and one site in the read-through translation (VEGF-A_x, see Table 1 and Supplementary file1, Fig. S5). Importantly, four out of the six positions in exon 8 are invariant at both DNA and protein level, thus technically preventing analysis, but indicating that purifying selection might be happening at the nucleotide level. The first amino acid of exon 9, whose corresponding nucleotides are part of the non-canonical splice acceptor consensus motif [71], showed evidence for diversifying selection. Not all exon 9 coding sequences terminate with a stop codon after 18 nucleotides. In about 10% of the analyzed mammalian sequences, the reading frame continues for 23–26 amino acids resulting in a predominantly basic tail, including a 4–7 amino acid long polyhistidine stretch (see Supplementary file1, Fig. S5c). To corroborate these results, we used SLAC analysis and confirmed evidence for purifying selection for one exon 8-site, one exon 9-site, and one exon 8 read-through-site (see Table 1). DIVAA analysis of the 3'-end of the VEGF-A gene showed high conservation of the nucleotide sequence within the coding region of

Table 1 Analysis of evolutionary selective pressures by comparing nonsynonymous and synonymous mutation rates in the coding sequences of VEGF-A exon 8, putative exon 9 and exon 8 read-through translation

	VEGF-A (Exon 8)	VEGF-A _{xxx} b (Exon 9)	VEGF-Ax (Exon 8 readthrough)
Consensus sequence (human sequence deviating from mammalian consensus are shown in BOLD and frequent reversals in <i>ITALICS</i>)	CDKPRR*	[SPC]LTRKD*	CDKPRR[*S] AG[QL]EEGASLRVSGTR[SP]LTRKD*
Positive (diversifying) selection shown in <i>ITALICS</i> , conservation (purifying selection) shown in BOLD	CDKPRR*	[SPC]LTRKD*	CDKPRR[*S] AG[QL]EEGASLRVSGTR[SP]LTRKD*
Fixed Effects Likelihood (FEL, p-values)	Pro-4 (6.2x10⁻⁵) Arg-5 (1.03x10⁻⁵)	<i>Ser-1 (0.0007)</i> Asp-6 (0.0002)	Pro-4 (2.4x10⁻¹¹) Ala-8 (8.3x10⁻⁵)
Single-Likelihood Ancestor Counting (SLAC, p-values)	Pro-4 (2.09x10⁻⁷)	Asp-6 (1.81x10⁻⁴)	Pro-4 (2.09x10⁻⁷)

Amino acid residue designations refer to the human sequence if not differently indicated. Differences in the p-value for the same amino acid residue result from intervening frameshift mutations (which are spliced out for VEGF-A_{xxx}b) and from differences in the reconstruction of the most likely ancestral sequences. Results were considered significant at $p < 0.001$, slightly more conservative than after the Bonferroni correction $p < (0.05/40)$. To analyze the VEGF-Ax sequence, the TGA stop codon at the end of exon 8 was replaced by the codon TCA to mimic read-through. In one out of the 149 analyzed sequences, this resulted in an in-frame stop codon, and the 3'-UTR sequences were removed to enable the analysis. Exon numbering is according to the canonical isoform (P15692-1), and the term "exon 9" is used according to Bates et al. [69]

exon 8 and 9 as well as within the exon 8 read-through sequence (Supplementary file1, Fig. S5a). Outside the coding sequences, nucleotide diversity is high and heterogeneous. We could explain some intronic heterogeneity by the leftovers of transposable elements (LINE, MER20B), which are present in some, but not other animal species.

Discussion

In this study, we have identified homologs of PDGFs/VEGFs in most animal phyla that show tissue organization (i.e., excluding sponges) and for which more than a few genome assemblies and gene predictions exist. Despite their pervasive occurrence in many branches of deuterostomes and protostomes, the data clearly support the notion that some animal phyla are completely or partially devoid of PDGF/VEGF-like molecules, and this might, above all, apply to clades with secondarily reduced body plans like Tunicata, or for the phyla Xenacoelomorpha or Dicyemida. Especially for many of the protostome phyla, not much genomic or mRNA data is available. Genome assemblies are often lacking, and the available prediction algorithms might not be very reliable as these animals are rarely the subject of genomic research. For these phyla, the lack of PDGF/VEGF-like proteins is a provisional hypothesis.

After hypothetical proteins are predicted from genomic sequences, programmatic bioinformatics workflows typically assign them to homology groups (e.g., using PANTHER [72]), resulting in automatic annotation like *PREDICTED*, *VEGF-C*. Despite this approach, many PDGF/VEGF homologs fail to be programmatically categorized into one of the 10 ortholog groups (*VEGF-A*, *PIGF*, *VEGF-B*,

VEGF-C, *VEGF-D*, *VEGF-F*, *PDGF-A*, *PDGF-B*, *PDGF-C*, *PDGF-D*). Our algorithm emulates crowd-sourcing by comparing uncategorized homologs to the most closely related manually and programmatically annotated PDGFs/VEGFs and establishes a majority opinion, allowing for the categorization of the majority of uncategorized vertebrate proteins into one of the ortholog groups. This crowd-sourcing combines human annotation of gene and protein records with the tree-building and clustering methodology used for the protein trees available at Ensembl (https://m.ensembl.org/info/genome/compara/homology_method.html), which are used for the automatic annotation.

Based on the phylogenetic tree of the animal kingdom and our analysis of PDGF/VEGF homologs in different animal clades, the emergence of the earliest PDGF/VEGF-like molecule ("proto-PDGF/VEGF") predates the establishment of the bilaterian body plan [73] and the split of the animal kingdom into deuterostome and protostome organisms before the start of the Cambrian about 540 MYA [74]. Intriguingly, this "proto-PDGF/VEGF" most likely featured a domain structure characteristic for the modern lymphangiogenic VEGF-C/VEGF-D subclass, having long N- and C-terminal extensions flanking the VHD and a characteristic repetitive cysteine residue pattern (the BR3P repeat) at its C-terminus. Concurrent with the relatively rapid evolution of different body plans during what has been termed the "Cambrian Explosion," the proto-PDGF/VEGF undergoes diversification establishing a VEGF-A-like and a VEGF-C-like branch and spinning off the PDGF branch. The deuterostome/protostome split predates both the VEGF diversification and the PDGF spinoff, which explains the difficulty of classifying PDGF/VEGF-like molecules on the protostome branch

(“*Drosophila* VEGFs,” “*C. elegans* VEGF-C”) as either PDGFs or VEGFs.

In the protostome branch, we can detect PDGF/VEGF-like factors (PVFs) in all but one clade for which substantial sequencing data are available. All 26 genome-sequenced flatworms seem to get along without any PVFs. Contrary to this, insects, mollusks, and segmented worms (Annelida) often feature more than one *Pvf* gene, whereas most nematodes feature only one. *C. elegans* PVF-1 is remarkable in that it is still—after more than 500 MYA of evolutionary separation—able to activate the human VEGF receptors-1 and -2 [38]. Protostome animals do not feature a cardiovascular system, with exceptions among mollusks and segmented worms (Annelida). The phylum Annelida contains species such as the earthworm *Lumbricus terrestris*, which features a closed circulatory system displaying vascular specialization and hierarchy, including a vessel-like heart with valves, larger blood vessels, capillaries, blood containing free hemoglobin, and a renal filtration system [75]. Until now, no protostome PVF has been shown to play any role in vascular development, and a unifying picture of PVF function in invertebrates has yet to emerge.

Whether this functional diversity reflects an absence of a cardiovascular system in the last common ancestor between vertebrates and invertebrates is unclear. A possible cardiovascular system in the last common ancestor did not necessarily require the existence of endothelial cells since the annelid cardiovascular system does not feature endothelial cells either [76]. In such a scenario, the cardiovascular system of vertebrates and invertebrates would be homologous, but endothelial cells would represent convergent evolution. However, some invertebrates feature endothelial-like cells [77, 78], and octopuses have molecular makeup surprisingly similar to vertebrates (e.g., VEGF receptors, Notch) [79]. Even the regulation of blood vessel formation in leeches was claimed to be inducible by human VEGF-A, arguing that perhaps even the endothelial cell was a feature of the last common ancestor of vertebrates and invertebrates [80]. In the invertebrate lineage, ECs are speculated to have developed from hemocytes [76], and also in vertebrates, such origin seems likely due to the close relationship of the hematopoietic and endothelial cell lineages, both featuring VEGF receptors and a common developmental origin [31, 81].

With PIGF, VEGF-B, VEGF-D, and VEGF-F, further specializations happen in both the VEGF-A and the VEGF-C lineage after the Cambrian period in the deuterostome branch. Instrumental for this specialization is most likely the VGD2, which doubled the number of PDGF/VEGF-like genes. When ignoring teleost fishes, whole-genome duplications are responsible for about half of the newly emerging PDGFs/VEGFs, the other half requiring duplication events at the gene or chromosome level (Fig. 4).

Echinodermata are the most simple animals that display PDGF/VEGF specialization at the gene level. The least complicated explanation for the existence of both VEGF-A-like and VEGF-C-like proteins in Echinodermata is that the first gene duplication of the proto-PDGF/VEGF happened prior to the VGD1. For the same reason, the separation of the PDGF lineage also likely predates the VGD1, resulting in PDGFs being present in cephalochordates (lancelets), which are the most simple organisms to have a pressurized vascular system in which the blood is moved around by peristaltic pressure waves created by contractile vessels [82]. In line with this notion is the important role of PDGFs in the supportive layers that stabilize blood vessels (pericytes, smooth muscle cells) [83].

Despite the availability of genome assemblies from six different tunicate species, the programmatic approach identified only one VEGF-like molecule in tunicates, *Ciona intestinalis*. This was surprising since there is prior data indicating the role of VEGF/VEGFR signaling in the circulatory system of tunicates [84]. However, the relationship between the receptor tyrosine kinase that was cloned from the tunicate *Botryllus schlosseri* and PDGF receptors, FGF receptors, and c-kit is not clear. The immunological detection used antibodies directed against human VEGFRs or VEGF-A, and the TK inhibitor PTK787 might have as well inhibited PDGF receptors and c-kit. Although the *C. intestinalis* VEGF-like growth factor appears most similar to VEGF-A, its phylogeny also allows descendance from the PDGF or VEGF-C branch. In that case, the similarity to VEGF-A might have originated from convergent evolution (“long branch attraction”). Since none of the other tunicate species seems to feature PDGF/VEGF homologs, horizontal gene transfer could be an alternative explanation.

Absence of PIGF and VEGF-B from entire animal vertebrate classes, VEGF-F more common than expected

Most striking was the absence of some VEGF family members from entire animal classes. We did not find any PIGF ortholog in Amphibia and also no VEGF-B ortholog in the clade Archosauria, which includes extant birds and crocodiles as well as extinct dinosaurs. Since bony fish feature both PIGF and VEGF-B, the absence of VEGF-B in extant Archosauria and PIGF in extant Amphibia likely represents an example of lineage-specific gene loss. While five avian protein sequences are annotated as “VEGF-B” or “VEGF-B-like” in the searched database, they did separate on a phylogenetic tree to the same branch as the VEGF-A sequences (data not shown). In addition, their genes did not show the typical exon–intron structure, which is characteristic of VEGF-B with overlapping open reading frames leading to two different protein sequences due to a frameshift [85].

As a counterpoint to the missing PIGF and VEGF-B, we observed, to our surprise, that VEGF-F is more common than generally thought. Discovered as a venom compound of vipers [21, 22], it was initially thought to be limited to venomous reptiles. However, we did detect VEGF-F-like sequences in non-venomous lizards and gekkos. VEGF-F is more or less pervasive throughout large parts of the lepidosaurian lineage, with occurrences in species so diverse as the Green anole and the Japanese gekko (which are located distantly from each other on the lepidosaurian tree). For this reason, VEGF-F likely evolved early on in the evolution of Lepidosauria prior to the invention of venom (Supplementary file1, Fig. S3). At this moment, it is unclear which functions VEGF-F might have originally fulfilled before it became co-opted as an integral viper venom component. In vipers, VEGF-F expression is highly restricted to the venom glands [86], where it acts by accelerating venom spread by inducing vascular permeability and by incapacitating the prey by lowering blood pressure. However, it is conceivable that VEGF-F still fulfills its original, non-venom function in the non-viper branch of the VEGF-F tree.

Complete absence of PDGFs/VEGFs

The absence of individual PDGFs/VEGFs from a species' proteome can be either real or only apparent due to incomplete sampling or an artifact of the bioinformatics analysis pipeline. We generally found very few exceptions to the clade-specific pattern of PDGF/VEGF occurrence in terrestrial vertebrates, which all featured the same set of PDGF/VEGF paralogs, confirming the reliability of the respective genome sequencing and gene prediction pipelines. In our programmatic screen, PDGF/VEGF-like sequences were apparently completely absent in some clades for two different reasons:

1. A lack of data (false negatives): PDGFs/VEGFs were apparently absent from clades where there was no comprehensive genomic data, or the genomic data had not been analyzed (e.g., sea spiders or velvet worms).
2. A true absence: PDGFs/VEGFs were absent from clades that are likely truly devoid of VEGF-like molecules (e.g., flatworms, where a substantial number of genomes have been sequenced and analyzed).

With increasing sequencing coverage, false negatives will disappear, as has happened for Cyclostomata during the writing of this manuscript. The occurrence of four PDGF/VEGF-like genes in Cyclostomata supports the currently largely accepted Early-1R hypothesis (i.e., that the VGD1 happened before the divergence of Cyclostomata). While recent data suggest an early hexaploidization event for the

Cyclostomata branch [87], we did not find evidence for more than four PDGF/VEGF genes in any cyclostomate genome.

Viral VEGFs

While many viruses indirectly induce angiogenesis [88], some viruses encode their own VEGF homologs. These proteins have been collectively termed “VEGF-E.” Viral VEGFs have been reported from parapoxviruses, which cause skin lesions in their respective mammalian hosts [89–91]. In these viruses, the VEGF-E gene is specifically responsible for swelling and vascular proliferation [92]. Based on the sequence homology to VEGF-A, VEGF-E is believed to have been captured from a host during viral evolution [90], similar to the *v-sis* oncogene, which is believed to be derived from captured host PDGF-B sequences [25]. Our database search confirms that viral VEGF homologs exist not only in four species of the parapoxvirus genus but also in the very distantly related megalocytiviruses, which infect fish [93]. Surprisingly, despite their non-overlapping host range, both the fish and mammalian viral VEGF-Es might originate from one single acquisition from a mammalian host. Unlike megalocytiviruses, which infect fish (and occasionally amphibians), parapoxviruses have a very broad mammalian host range, which occasionally includes humans but is mostly covering domesticated and wild ungulates [94, 95]. While parapoxvirus infections are typically self-limiting, megalocytiviruses cause considerable economic damage to aquaculture. The pathophysiology of megalocytiviral diseases is not well understood. The infection leads to perivascular cell hypertrophy [96], and VEGF-E might facilitate virus dissemination via increasing vascular permeability.

The “silk homology” domain (SHD)

Aligning the VEGFs' accessory domains is non-trivial as they contain a variable number of repeats. Especially the evolutionary history of the SHD of VEGF-C and VEGF-D is perhaps impossible to deduce with reasonable accuracy because it consists of several complete and incomplete Balbiani ring-3 protein (BR3P) repeats. The C-terminal tails of VEGF-A₁₆₅ and VEGF-B₁₆₇ show a reduced number of repeats, and for VEGF-A, this domain was named “heparin-binding domain” (HBD). “Heparin-binding” or binding to the extracellular matrix (ECM) and cell surfaces is one function of the SHD [97], and the HBDs of VEGF-A₁₆₅ and VEGF-B₁₆₇ have developed a stronger heparin affinity compared to VEGF-C or VEGF-D, which may have allowed for their size reduction. In addition, the SHD also keeps VEGF-C inactive, likely by sterical hindrance [98], which is not required for the longer VEGF-A isoforms, whose HBD can mediate inactivity by sequestration [99]. However, some signaling appears possible when ECM-bound VEGF-A₁₈₉ or

VEGF-A₂₀₆ are in direct contact with endothelial cells [100]. Also, ECM-associated VEGF-A₁₆₅ can signal, although distinctly from free VEGF-A₁₆₅ [101, 102]. Our analysis shows that the SHD was likely an essential part of the proto-PDGF/VEGFs. Despite the SHD being larger than the receptor-activating VHD, it has been maintained for hundreds of millions of years. Since much shorter propeptides can achieve protein inactivity, we suspect an additional function for this domain: establishing a VEGF-C gradient.

VEGF-A gradients are instrumental in vascular network patterning [103–105]. They are believed to result from the interaction of the longer VEGF-A isoforms with ECM and cell surfaces and to be essential for embryonic vascularization [106, 107]. Although VEGF-A₁₆₅ is considered the major isoform in humans [108], the stronger ECM-binding VEGF-A₁₈₉ and other long isoforms dominate sequence databases. Splice prediction algorithms do not even predict the existence of VEGF-A₁₆₅ (and sometimes VEGF-A₁₂₁) for numerous animals such as cattle, horses, and many birds (data not shown). In addition to mRNA splicing, teleost fish have diversified VEGF-A by gene duplication. Both zebrafish VEGF-As (Vegfaa and Vegfab) are indispensable [109]. While comparable in length, they differ significantly in their charge, but whether this translates into a differential interaction with the ECM is unknown.

Two splice isoforms might be specific to mammals: VEGF-A_{XXXb} and VEGF-Ax. VEGF-A_{XXXb} isoforms are generated by using a non-canonical splice acceptor site in exon 8, thus changing the last 6 amino acids of the protein [69]. In contrast, VEGF-Ax isoforms are generated by translational read-through within exon 8. Unlike VEGF-A_{XXXb}, VEGF-Ax contains the same 6 C-terminal amino acid residues as the canonical VEGF-A isoforms but extended by another 22 amino acid residues (see Supplementary file1, Figure S5c) [70].

Both VEGF-A_{XXXb} and VEGF-Ax have been reported to be antiangiogenic [69, 70, 110]. Others have shown weak angiogenic potential of VEGF-Ax, which resulted from reduced or abolished interaction with NRP-1 [111], an important co-receptor in the context of angiogenesis [112]. Since exon 8-derived sequences are crucial for NRP-1 interaction [113, 114], VEGF-A_{XXXb} would fail to interact due to the lack of these sequences, and VEGF-Ax due to active interference mediated by the read-through tail. If VEGF-Ax binding to VEGFR-2 remained strong, VEGF-Ax could displace VEGF-A from VEGFR-2, eliminate the NRP-1 contribution, and act as a partial agonist suppressing angiogenesis, e.g., in a high-VEGF-A environment [115]. However, experiments failed to observe such competition [111].

Our data cannot inform about the functional characteristics of these isoforms but confirm that exon 8 of VEGF-A is strongly conserved at the DNA level. There is some evidence for VEGF-A_{XXXb} and VEGF-Ax being under

purifying selection at the protein level. However, while the conservation of protein-coding sequences is mostly enforced at the protein level, RNA constraints can mimic protein conservation [116], especially perhaps for short sequences. In line with the latter explanation are reports that dispute the existence of inhibitory isoforms altogether [117, 118]. Interestingly, the diversifying selection of the first amino acid of exon 9 (serine/proline) manifests in its frequent conversion to cysteine, which is observed in several species (e.g., bonobos, sheep, alpaca, camels). It is tempting to speculate whether this reversal to cysteine would affect the angiogenic potency of VEGF-A_{XXXb}.

How did the complex splicing landscape of *VEGF-A* evolve? Likely, transposable elements played a role [119]. The effect of a retrotransposon insertion (long interspersed nuclear element, LINE) during mammalian evolution can clearly be seen in the *VEGF-A* intron preceding exon 8 (Supplementary file1, Fig. S5a). Transpositions and subsequent deletions and rearrangements resulted in rather large differences in the length and internal intron structure of *VEGF-A* genes of different species. Also interesting, although not rare in the human genome, is that the same intron harbors the remnants of a MER20B transposable element, which is a mammal-specific progesterone-responsive enhancer instrumental in the regulatory network necessary for pregnancy [120].

Similar to VEGF-A, VEGF-C might form gradients by the interaction of its SHD domain with the ECM [97]. Such morphogenetic gradients might be crucial for developmental lymphangiogenesis but also for developmental angiogenesis and vasculogenesis [51, 121, 122], possibly explaining the strong purifying selection of VEGF-C in its VHD and SHD. Also, all other VEGFs, except for PlGF, showed strong conservation in the VHD (Supplementary file1, Fig. S6). For the VEGF-A isoforms, the sequence diversity outside the VHD increased with the length of the isoform (Supplementary file1, Fig. S3), perhaps facilitated by the existence of many isoforms.

Structural differences between protostome and deuterostome PDGFs/VEGFs

PDGF/VEGFs form a family within the superfamily of cystine knot growth factors. Their hallmark is a characteristically spaced pattern of eight cysteine residues, consisting of the 6-cysteine pattern of the cystine knot signature expanded by two cysteines responsible for the covalent dimer formation of PDGFs/VEGFs [123]. The 8-cysteine pattern is broken with respect to the intermolecular disulfide bond-forming cysteine by only one vertebrate member of the PDGF/VEGF family, PDGF-C. However, in protostomes, missing intermolecular disulfide bonds are the rule rather

than the exception (Fig. 2). While disulfide bridges increase thermostability, low ambient water temperatures are typical for many freshwater and marine species, for which covalent dimer formation via disulfide bonds might not have any advantage over noncovalent dimer formation, while disulfide bond formation comes at a cost [124, 125]. Even at 37 °C, the cystine bridge is not strictly necessary for dimer formation: VEGF-C also forms noncovalent dimers [19], and stable VEGF-A can also be produced after the mutation of the intermolecular cystine bridge-forming cysteines [126].

Conserved when present, not needed when absent

Different from VEGF-A and VEGF-C, which are pervasively maintained within the vertebrate lineage, PIGF and VEGF-B are absent from major vertebrate classes. PIGF appears to be absent in amphibians, and VEGF-B is completely missing from birds and crocodiles. The gene duplication that led to the establishment of the PIGF and VEGF-B genes presumably happened shortly before the cartilaginous fishes branched off. Consequently, e.g., shark VEGF-B is much more similar to VEGF-A compared to VEGF-B of land animals (Supplementary file1, Fig. S7).

The absence of PIGF in amphibians and VEGF-B in birds and crocodiles is due to secondary gene loss events, which were apparently—very similar to knockout experiments of the same genes in mice [12–14]—well tolerated. While VEGF-B has been proposed to play a role in the regulation of endothelial fatty acid uptake [127] and vascularization and tissue perfusion via indirect activation of VEGFR-2 [128], its precise role remains controversial [129, 130]. Its evolutionary loss might have been a net benefit for birds, perhaps even instrumental to enabling the high metabolic turnover needed for flight [131]. In any case, our understanding of PIGF, VEGF-B, and VEGF-D, all having been conserved for 500 MYA despite their apparent present-day redundancy in mice, leaves ample room for future insights.

While very common in plants, polyploidy is rare among animals. Among vertebrates, it is tolerated best by fish and amphibians [132]. This tolerance is also seen at the gene level. We frequently found individual *pdgf/vegf* gene duplications in fish but not in higher vertebrates. Holostei fish, a sister clade of the teleost fish, show, for example, a duplicated *vegfc* gene. Whether the duplicated *vegfc* genes have been maintained in Holostei from one of the prior whole-genome duplications or whether they resulted from a limited gene duplication event early in the Holostei lineage is unknown and perhaps unknowable since the chromosomal context has likely been already lost. Surprisingly, both *vegfc* genes continue to be strongly conserved in Holostei. The conservation is strongest in the receptor binding domain but can also be seen in the SHD (Fig. 6b). Interestingly, only two of the conserved residues of the PDGF/VEGF signature

were under strong purifying selection, and only three out of the nine residues under strong purifying selection were cysteines, arguing that a better, perhaps more sensitive search pattern for the detection of PDGF/VEGF proteins could be developed by taking conserved non-cysteine residues into consideration. Contrasting this strong conservation is the variability of the immediately N-terminally adjacent region, which is presumably instrumental in the activation of the inactive pro-VEGF-C into the mature VEGF-C by proteolysis [133] (see also <https://elifesciences.org/articles/44478/figures#fig2s2>). Another gene duplication example is the loach *Triplophysa rosa* (Fig. 6d), which features three *vegfa* and two *pgf* genes, both of which could be de-novo duplicated or maintained from one of the previous WGDs.

Evolutionary recent whole-genome duplications have been reported for catostomid fishes such as the Chinese Sucker (*Myxocyprinus asiaticus*) [134, 135] and the common carp (*Cyprinus carpio*) [136, 137]. It would be interesting to analyze the pseudogenization pattern for PDGF/VEGF genes in these two species.

Fish as model organisms

Teleost fish, which comprise most of the extant fish species, have undergone a lineage-specific whole-genome duplication 350 MYA [52, 138], which resulted in presumably ten active *vegfa* and eight active *pdgfb* genes immediately after the duplication. In the teleost zebrafish, at least 13 of the duplicated *pdgf/vegf* genes remain functional until today, according to our analysis (*pdgfaa/ab*, *pdgfbba/bb*, *pdgfc*, *pdgfd*, *vegfaa/ab*, *pgfa*, *pgfb*, *vegfbba*, *vegfc*, *vegfd*). While the Ensemble genome database also lists *vegfbba* as an active zebrafish gene, we did not find any mRNA transcript matching it in 21 fish species, including zebrafish. *Vegfbba* might therefore be a pseudogene, or it was simply not expressed in the tissues that were used for mRNA extraction.

Different teleost lineages underwent distinct gene elimination patterns; this is the most simple explanation for the occurrence of, e.g., two *vegfc* genes in the European eel (order *Anguilliformes*) or the butterflyfish (order *Osteoglossiformes*). Salmonids, on the other hand, have undergone one additional full-genome duplication approximately 88 MYA [54]. While this might have resulted in theoretically 36 different active *pdgf/vegf* genes immediately after the duplication, not all of these are active today. For the salmonid *Salmo trutta* (Brown trout), 26 of these genes are identified by the Ensemble analysis pipeline as active (https://www.ensembl.org/Salmo_trutta/Location/Genome?ftype=Domain;id=IPR000072), and for 21 of them, we found mRNA transcripts. However, if mRNA and protein data are absent, it is not always possible to reliably distinguish functional from pseudogenes [139].

The large difference in the heterogeneity of the PDGF/VEGF repertoire between fishes and terrestrial vertebrates is reflected in the heterogeneity that can be seen at the anatomical and functional levels of the vasculature in different fishes. Transdifferentiation of lymphatic vessels into blood vessels has been seen so far only in fishes [51], and it will be interesting to see which molecular signals underly the transdifferentiation and the establishment of the connections of this specialized secondary vasculature to the primary circulation. However, the partial loss of gene function within the teleost lineage remains challenging for experimental fish—and specifically zebrafish—research. Multiple functions that were prior to the genome duplication executed by a single protein (e.g., VEGF-A) might be executed by two (zebrafish) or even more (Salmonidae, Catostomidae, *Cyprinus carpio*) ohnologs. There is multiple evidence that the two zebrafish ohnologs *vegfaa* and *vegfab* have diversified in terms of mRNA splicing and, consequently, their angiogenic properties [109, 140, 141]. Similarly, the ohnologs *vegfc* and *vegfd* have diversified differently in fishes compared to terrestrial animals in tissue distribution and receptor interaction [142, 143]. While this makes fish models at times more tedious and difficult to interpret compared to mouse models [144], it is at the same time a unique opportunity to discover and understand a morphological and physiological diversity unknown in mammals [51, 145].

Materials and methods

Comprehensive database scan

BLAST searches were executed for a set of 13 reference proteins (human PDGF-A/-B/-C/-D, PIGF-3, VEGF-A_{121/165/206}, VEGF-B_{167/186}, VEGF-C/-D, and vammin-1) against the non-redundant NCBI protein database (corresponding to RefSeq Release 94). According to the Hit_def of each result, a hit was programmatically categorized based on the Hit_def field in the blast result as a *synonymous hit* (e.g., when the VEGF-D search results in a hit annotated with “VEGF-D” or “FIGF”), a *related hit* (e.g., when a VEGF-D search results in a hit annotated with “VEGF-B” or “PDGF”) or an *undefined hit* (e.g., when a search for VEGF-D results in a hit annotated with “hypothetical protein” or similar). To categorize undefined hits, secondary BLASTS were initiated with the sequences for undefined hits, and if more than 50% of the secondary hits agreed in their annotation on a specific PDGF/VEGF, this information was used to categorize the primary hit. The 50% threshold had been empirically determined to be conservative, i.e., never resulting in false negative categorizations with a known set of VEGFs. Undefined hits in secondary BLASTS results are assigned to specific PDGFs/VEGFs in the same fashion but using

computationally more expensive RPS BLAST instead of protein blast. The flow chart of the analysis is shown in Supplementary file1, Fig. S1.

The full table of BLAST results (Supplementary Table 1) was assembled programmatically from the data generated as described above, and the number of distinct animal species for each clade was obtained from the NCBI taxonomy database. “Fully sequenced” genomes were loosely defined as those that had registered a BioProject with NCBI with the data type “Genome sequencing” or “Genome sequencing and assembly” in the group “animals” and for which results had been published (1049 species at the time of this writing). The number of protein sequences published for a specific clade was the number of sequences in the corresponding taxon-specific subsection of the NCBI protein database. For all clades with less than 200 unique VEGF homologs, all primary BLAST hits were manually checked for false positives (i.e., when the human-curated protein description specified a named non-PDGF/VEGF protein in the sequence description). The formula for background coloring of Fig. 1 and Supplementary Table 1 according to the heuristic reliability due to biased sampling was:

$$reliability = \log_{10} \left(\frac{\text{number of fully sequenced genomes}^{2.5}}{\text{number of animal species} \cdot \text{number of protein sequences} + 1} \right)$$

Alignment, phylogenetic tree building, and conservation analysis

Alignment of cnidarian with human PDGFs/VEGFs (Fig. 2)

The mcoffee mode of T-coffee 12.00 was used to align a representative subset of 10 cnidarian PDGF/VEGF-like sequences from all six species in which PDGF/VEGF-like sequences were identified, all seven human PDGF/VEGF orthologs, *C. elegans* PVF-1, and *Drosophila* PVF2. The alignment was trimmed down to 130 amino acid residues of the consensus sequence (corresponding to the VHD) starting from the first of the eight conserved cysteines of the PDGF/VEGF signature (until Proline-132 from VEGF-A). During the alignment, all conserved cysteine residues were anchored according to the alignment by Heino et al. [35].

Assessing the relationships between vertebrate and invertebrate PDGFs/VEGFs (Fig. 3)

The alignment from Fig. 2 above was expanded by including all four PDGFs/VEGFs identified in *Hydra vulgaris*, all three *Drosophila* PVFs, all human PDGF/VEGF paralog, and the PDGF/VEGF-like molecule identified in the parasite *Brugia malayi*. The TGF- β homolog of *C. elegans* UNC129 was used as an outgroup. To capture information about the ancillary domains/propeptides of the proteins, the sequences included in the alignment were expanded amino-terminally by 20 amino acids and C-terminally by 30 amino

acids beyond the conserved eight cysteine residues of the PDGF/VEGF signature. The mcoffee-provided alignment was trimmed to include 179 amino acid positions corresponding to the first amino acid of the major mature form of human VEGF-C [19] until the last cysteine of the first repeat of the BR3P motif (C-X₁₀-C-X-C-X_(1,3)-C) [15]. Tree building was performed with PhyML 3.0 [146], combining both the original PhyML algorithm and subtree pruning and regrafting for tree topology search. To estimate the reliability of branches, 1000 bootstrapping replicates were performed. The tree was visualized with FigTree version 1.4.4, exported to an SVG file, and visually enhanced using Inkscape (<https://inkscape.org>).

Holostei VEGF-C analysis (Fig. 6a–c)

The amino acid alignment and tree building for Holostei VEGF-Cs and VEGF-Ds were performed as described above using T-coffee and PhyML. As an outgroup sequence for tree rooting, we used PDGF-A from one of the Holostei species (*Lepisosteus oculatus*). The corresponding mRNA alignment was generated with PAL2NAL. Treefile and alignment were used by HyPhy version 2.5.1 [147] to test for pervasive site-level selection (SLAC). The graphs were generated from the json files using Gnumeric. The alignment of the VHD of representative VEGF-C sequences below the detailed conservation view was generated from an aligned Fasta file with SnapGene Viewer 6.1.1.

Tree building for *Triplophysa rosa* PDGFs/VEGFs (Fig. 6d)

All 11 PDGF/VEGF sequences identified for the sucker *T. rosa* were aligned, and tree building was performed as described above. For this analysis, we did not include any outgroup resulting in an unrooted tree.

Analysis of viral VEGF homologs

A PSI-BLAST limited to the taxon Viridae (taxid:10,239) was run against the starting sequence AAD03735.1 (vascular endothelial growth factor homolog VEGF-E from Orf virus) until no new sequences were found above the 0.005 threshold. The Fasta descriptions were adjusted to include virus names and host species. For each host species, the VEGF-A₁₆₅, PIGF-1, and VEGF-B₁₈₆ orthologous protein sequences were retrieved (if available) and included in the alignment and tree building, which was performed as described above. Only three out of the eight fish VEGF-B sequences were available. Therefore, we included both zebrafish VEGF-B sequences in the analysis. Similarly, no VEGF sequences were available for *Halichoerus gryp*

(gray seal). These were replaced with sequences from the closest species for which VEGF sequences were available (*Zalophus californianus*, California sea lion). The protein sequence alignment was performed with T-coffee, the tree building with PhyML, and the visualization of the tree with the ETE Toolkit 3.0. The v-sis sequences from the Simian sarcoma virus were used as an outgroup to root the tree. The workflow and all sequences used for the analysis are available from GitHub as a python script (<https://github.com/mjeltch/VEGF>). Tree topology was used to infer the likely origin(s) of viral VEGFs.

Analysis of VEGF-F origin

A tree was constructed with T-coffee and PhyML using 15 snake venom VEGFs and the hemangiogenic VEGFs from four bird species, eight mammals, eleven reptiles, and two amphibians, for which a complete set of proteins was available (excluding VEGF-B in birds and crocodiles and PIGF in amphibians). The tree was visualized with iTOL v5 [148] and enhanced using Inkscape.

Comparison of conservation levels between individual VEGFs

To compare the degree of conservation and to identify possible positive selection, codon analysis (synonymous versus nonsynonymous changes) was deployed. Reference protein and transcript sequences for available ortholog sets were downloaded from NCBI (<https://www.ncbi.nlm.nih.gov/gene/XXXX/ortholog>, XXXX = 7422, 7423, 7424, 2277, 5228 for VEGF-A, -B, -C, -D and PIGF, respectively). Obviously bogus or truncated transcript predictions (lacking essential exons of the PDGF/VEGF homology domain or being of low quality) were eliminated manually from the set. Several proteins/transcripts had to be replaced manually to ensure that only transcripts of the same isoform were compared since not all species feature the same set of isoforms (e.g., for VEGF-C: *Sus scrofa*, for VEGF-A: *Mus musculus*). Species were only included if they featured the full set of five mammalian VEGFs in the database (VEGF-A, PIGF, VEGF-B/-C/-D). The full list (sets of 5 VEGF paralogs for 82 species) was reduced to comprise only the 50 most informative sequences using T-coffee [149]; however, all sequences in a set were maintained if only one sequence in a set had been classified as informative. The full set of protein and mRNA sequences is available in Fasta format as Supplementary data. The protein sequences of each VEGF ortholog were aligned using T-coffee's mcoffee mode [150]. The final alignments were trimmed manually (keeping the sequence from the first to the last cysteine of the PDGF/VEGF cysteine signature plus 15 amino acid residues N-terminally and 5 amino acid residues C-terminally). To prepare

the protein alignment for the analysis of pervasive purifying/adaptive evolution, the corresponding mRNA alignment was obtained with PAL2NAL 14 [151]. A maximum-likelihood (ML) approach was used to infer nonsynonymous versus synonymous substitution rates on a per-site basis for the alignment [152], using SLAC (Single-Likelihood Ancestor Counting) from the HyPhy 2.5.1 software package. The graph was generated with the Python library Seaborn 0.10 and enhanced via Inkscape with a molecular ribbon model of VEGF-C generated by Pymol 2.3.0 based on the PDB structure 2X1X.

Cladograms of evolutionary PDGF/VEGF history

A tree file for the animal kingdom was downloaded from the Open Tree of Life (<https://tree.opentreeoflife.org>), which maintains a consensus tree obtained by semi-automated synthesis of many individual studies [44] (<https://tree.opentreeoflife.org/curator>). This treefile was used programmatically by the ETE Toolkit to generate Fig. 1 and Supplementary Table 1. To generate Fig. 4, a cladogram was generated from the same file, excluding the protostome branch with FigTree version 1.4.4. The PDF-exported tree was enhanced using Inkscape. When public-domain animal silhouettes were available, they were obtained from PhyloPic (<http://phylopic.org>); otherwise, they were drawn by the authors.

Determination of absence of VEGF-B genes in birds

Because we had not come across any avian VEGF-B sequence, we started by blasting the Entrez protein database [153] with a reptilian VEGF-B protein sequence (Chinese softshell turtle VEGF-B, Uniprot K7FWR8). The sequence ids of all hits were re-written to include the animal class and common name of the organism to facilitate the identification of potential avian VEGF-B sequences. This set of 4976 sequences was subjected to multiple sequence alignment (MSA) using mcoffee. Gblocks was used with the following in order to manually curate the alignment [154]. After converting the output with Dendroscope 3.8.4 to Newick format, the graphical representation was generated with iTOL [148], visually refined using Inkscape, and inspected for avian VEGF-B sequences. In order not to miss distantly related sequences, we repeated the above analysis but used three rounds of a PSI-BLAST, based on all available VEGF-B sequences and all avian VEGF-A and PIGF sequences.

Fish mRNA analysis

The PhyloFish mRNA database (<http://phylofish.sigenae.org>) was queried using tblastn with all *Danio rerio* PDGF/VEGF protein sequences, resulting in 1547 unique transcripts. mRNA sequences were downloaded for all transcripts. 405

of these transcripts were identified as PDGF/VEGF family members with a relaxed PDGF signature (using the regular expression P.?C.{2,8}C.?G.?C). Individual phylogenetic trees were built for the PDGF/VEGF transcriptome of each species using *Danio rerio* PDGFs/VEGFs as reference sequences. Unannotated mRNA sequences were classified manually based on the nearest reference sequence neighbor on the tree. The total number of unique mRNA transcripts for each species and the number of unique transcript contigs were tabulated using Gnumeric version 1.12.46 (Supplementary Table 3). The numbers were normalized to zebrafish, for which 48,158 unique mRNA transcripts had been obtained. The data were visualized using the Gnumeric Matrix plot function. The plot was visually enhanced in Inkscape with a cladogram based on [52]. For the extended mRNA analysis (Supplementary file1, Fig. S8), which compares mRNA levels of different organs within one fish species, expression levels were not normalized.

Quantification of diversity and VEGF-A_{xxx}b/VEGF-Ax selection

As the DIVAA software could not be retrieved anymore, we reimplemented the algorithm in Biopython based on the publication [68]. As an input to the DIVAA algorithm, VEGF-A isoforms were programmatically determined, but VEGF-B isoforms were manually assigned because fishes were found to have a single VEGF-B isoform which displays features of both mammalian isoforms simultaneously, having a basic stretch C-terminally to the VHD, followed by a hydrophobic region and a terminal, basic, cysteine-rich region. For other VEGFs, different isoforms were not separately analyzed.

To analyze whether the sequences coding for exon 8 of VEGF-A, exon 9 of VEGF-A_{xxx}b, and the read-through translation of exon 8 are under evolutionary selection, we inferred nonsynonymous and synonymous substitution rates using a maximum-likelihood approach (FEL) and the SLAC (Single-Likelihood Ancestor Counting) approach [152]. Since this method works only on protein-coding sequences, we additionally adapted DIVAA [68] for the analysis of nucleotide sequences for a simple measure of the diversity and conservation beyond the translated part of the 3'-end of the VEGF-A mRNA. The amino acid residues of the DIVAA analysis are replaced in the modified algorithm by the five possible states of a position in a nucleotide sequence alignment (A, T, G, C, -/gap).

An alignment was generated for 148 mammalian VEGF-A sequences covering the area equivalent to nucleotides 19,294–19,443 of the human VEGF-A reference sequence gene (NG_008732.1). The sequences coding for exon 8 of VEGF-A, exon 9 of VEGF-A_{xxx}b, and the read-through

translation of exon 8 were extracted for SLAC analysis, which used a phylogenetic tree generated over a larger 3'-region due to the short length of the coding sequences to analyze. The equivalent 3'-region of the *VEGF-C* gene was analyzed as a comparison.

Supplementary Information The online version contains supplementary material available at <https://doi.org/10.1007/s10456-023-09874-9>.

Acknowledgements We thank Jeremy Pasquier et al. for access to the fish mRNA sequencing data. We also wish to acknowledge CSC—IT Center for Science, Finland, for the provisioning of computational resources.

Author contributions KR and MJ analyzed and interpreted the data and drafted, wrote, and edited the manuscript. MJ developed and performed the bioinformatics analyses, acquired funding, and supervised the study. HB performed the phylogenetic analyses. KR manually curated programmatically uncategorized data.

Funding Open access funding provided by University of Helsinki including Helsinki University Central Hospital. This research was funded by the Päivikki and Sakari Sohlberg Foundation, the Novo Nordisk Foundation (#21036), and the Academy of Finland (#337120). M.J. was supported by the Paulo Foundation and the Einar and Karin Stroem Foundation for Medical Research. K.R. was supported by the Otto A. Malm Foundation. H.B. was supported by the Finnish National Agency for Education (EDUFI) and the Finnish Pharmaceutical Society.

Data availability All of the data used for this study are available from the corresponding GitHub repositories. The original search results are online at: https://mjlab.fi/3Hm8PaB9Kee_usD1xll/animalia.svg.

Code availability Scripts and algorithms used in this study are available from the following GitHub repositories: <https://github.com/mjeltsch/VEGFE>; <https://github.com/mjeltsch/Holostei>; <https://github.com/mjeltsch/VEGFphylo>; <https://github.com/mjeltsch/cnidariaVEGFs>; <https://github.com/mjeltsch/VEGFselect>; https://github.com/mjeltsch/Fish_mRNA; <https://github.com/mjeltsch/divaa>.

Declarations

Conflict of interest The authors declare no competing interests.

Open Access This article is licensed under a Creative Commons Attribution 4.0 International License, which permits use, sharing, adaptation, distribution and reproduction in any medium or format, as long as you give appropriate credit to the original author(s) and the source, provide a link to the Creative Commons licence, and indicate if changes were made. The images or other third party material in this article are included in the article's Creative Commons licence, unless indicated otherwise in a credit line to the material. If material is not included in the article's Creative Commons licence and your intended use is not permitted by statutory regulation or exceeds the permitted use, you will need to obtain permission directly from the copyright holder. To view a copy of this licence, visit <http://creativecommons.org/licenses/by/4.0/>.

References

- Blair JE, Hedges SB (2005) Molecular phylogeny and divergence times of deuterostome animals. *Mol Biol Evol* 22:2275–2284. <https://doi.org/10.1093/molbev/msi225>
- Benton MJ (1990) Phylogeny of the major tetrapod groups: Morphological data and divergence dates. *J Mol Evol* 30:409–424. <https://doi.org/10.1007/BF02101113>
- Sereno PC (1999) The evolution of dinosaurs. *Science* 284:2137–2147. <https://doi.org/10.1126/science.284.5423.2137>
- Lawrence MG, Lai J, Clements JA (2010) Kallikreins on steroids: structure, function, and hormonal regulation of prostate-specific antigen and the extended kallikrein locus. *Endocr Rev* 31:407–446. <https://doi.org/10.1210/er.2009-0034>
- Mural RJ, Adams MD, Myers EW et al (2002) A comparison of whole-genome shotgun-derived mouse chromosome 16 and the human genome. *Science* 296:1661–1671. <https://doi.org/10.1126/science.1069193>
- Vitt UA, Hsu SY, Hsueh AJW (2001) Evolution and classification of cystine knot-containing hormones and related extracellular signaling molecules. *Mol Endocrinol* 15:681–694. <https://doi.org/10.1210/mend.15.5.0639>
- Mattonet K, Jeltsch M (2015) Heterogeneity of the origin of the lymphatic system. *Lymphol Forsch Prax* 19:84–88
- Risau W (1997) Mechanisms of angiogenesis. *Nature* 386:671–674. <https://doi.org/10.1038/386671a0>
- Simons M, Gordon E, Claesson-Welsh L (2016) Mechanisms and regulation of endothelial VEGF receptor signalling. *Nat Rev Mol Cell Biol* 17:611–625. <https://doi.org/10.1038/nrm.2016.87>
- Carmeliet P, Ferreira V, Breier G et al (1996) Abnormal blood vessel development and lethality in embryos lacking a single VEGF allele. *Nature* 380:435–439. <https://doi.org/10.1038/380435a0>
- Ferrara N, Carver-Moore K, Chen H et al (1996) Heterozygous embryonic lethality induced by targeted inactivation of the VEGF gene. *Nature* 380:439–442. <https://doi.org/10.1038/380439a0>
- Aase K, von Euler G, Li X et al (2001) Vascular endothelial growth factor-B-deficient mice display an atrial conduction defect. *Circulation* 104:358–364. <https://doi.org/10.1161/01.CIR.104.3.358>
- Bellomo D, Headrick JP, Silins GU et al (2000) Mice lacking the vascular endothelial growth factor-B gene (*Vegfb*) have smaller hearts, dysfunctional coronary vasculature, and impaired recovery from cardiac ischemia. *Circ Res* 86:E29–35. <https://doi.org/10.1161/01.res.86.2.e29>
- Tayade C, Hilchie D, He H et al (2007) Genetic deletion of placenta growth factor in mice alters uterine NK cells. *J Immunol* 178:4267–4275. <https://doi.org/10.4049/jimmunol.178.7.4267>
- Joukov V, Pajusola K, Kaipainen A et al (1996) A novel vascular endothelial growth factor, VEGF-C, is a ligand for the Flt4 (VEGFR-3) and KDR (VEGFR-2) receptor tyrosine kinases. *EMBO J* 15:290–298. <https://doi.org/10.1002/j.1460-2075.1996.tb00359.x>
- Orlandini M, Marconcini L, Ferruzzi R, Oliviero S (1996) Identification of a C-FOS-induced gene that is related to the platelet-derived growth factor/vascular endothelial growth factor family. *Proc Natl Acad Sci U S A* 93:11675–11680. <https://doi.org/10.1073/pnas.93.21.11675>
- Jeltsch M, Kaipainen A, Joukov V et al (1997) Hyperplasia of lymphatic vessels in VEGF-C transgenic mice. *Science* 276:1423–1425. <https://doi.org/10.1126/science.276.5317.1423>
- Jeltsch M, Jha SK, Tvorogov D et al (2014) CCBE1 enhances lymphangiogenesis via a disintegrin and metalloprotease with thrombospondin motifs-3-mediated vascular endothelial growth

- factor-C activation. *Circulation* 129:1962–1971. <https://doi.org/10.1161/CIRCULATIONAHA.113.002779>
19. Joukov V, Sorsa T, Kumar V et al (1997) Proteolytic processing regulates receptor specificity and activity of VEGF-C. *EMBO J* 16:3898–3911. <https://doi.org/10.1093/emboj/16.13.3898>
 20. Ogawa S, Oku A, Sawano A et al (1998) A novel type of vascular endothelial growth factor, VEGF-E (NZ-7 VEGF), preferentially utilizes KDR/Flk-1 receptor and carries a potent mitotic activity without heparin-binding domain. *J Biol Chem* 273:31273–31282. <https://doi.org/10.1074/jbc.273.47.31273>
 21. Komori Y, Sugihara H (1990) Purification and physiological study of a hypotensive factor from the venom of *Vipera aspis aspis* (aspic viper). *Toxicol* 28:359–369. [https://doi.org/10.1016/0041-0101\(90\)90073-G](https://doi.org/10.1016/0041-0101(90)90073-G)
 22. Komori Y, Nikai T, Taniguchi K et al (1999) Vascular endothelial growth factor VEGF-like heparin-binding protein from the venom of *Vipera aspis aspis* (aspic viper). *Biochemistry* 38:11796–11803. <https://doi.org/10.1021/bi990562z>
 23. Yamazaki Y, Matsunaga Y, Tokunaga Y et al (2009) Snake venom vascular endothelial growth factors (VEGF-Fs) exclusively vary their structures and functions among species. *J Biol Chem* 284:9885–9891. <https://doi.org/10.1074/jbc.M809071200>
 24. Hughes AL, Irausquin S, Friedman R (2010) The evolutionary biology of poxviruses. *Infect Genet Evol J Mol Epidemiol Evol Genet Infect Dis* 10:50. <https://doi.org/10.1016/j.meegid.2009.10.001>
 25. Doolittle RF, Hunkapiller MW, Hood LE et al (1983) Simian sarcoma virus onc gene, v-sis, is derived from the gene (or genes) encoding a platelet-derived growth factor. *Science* 221:275–277. <https://doi.org/10.1126/science.6304883>
 26. Kipryushina YO, Yakovlev KV, Odintsova NA (2015) Vascular endothelial growth factors: a comparison between invertebrates and vertebrates. *Cytokine Growth Factor Rev* 26:687–695. <https://doi.org/10.1016/j.cytogfr.2015.04.001>
 27. Singh JP, Chaikin MA, Stiles CD (1982) Phylogenetic analysis of platelet-derived growth factor by radio-receptor assay. *J Cell Biol* 95:667–671. <https://doi.org/10.1083/jcb.95.2.667>
 28. Grassot J, Gouy M, Perrière G, Mouchiroud G (2006) Origin and molecular evolution of receptor tyrosine kinases with immunoglobulin-like domains. *Mol Biol Evol* 23:1232–1241. <https://doi.org/10.1093/molbev/msk007>
 29. Hoch RV, Soriano P (2003) Roles of PDGF in animal development. *Development* 130:4769–4784. <https://doi.org/10.1242/dev.00721>
 30. Yan Y, Hillyer JF (2020) The immune and circulatory systems are functionally integrated across insect evolution. *Sci Adv* 6:eabb3164. <https://doi.org/10.1126/sciadv.abb3164>
 31. Eichmann A, Corbel C, Nataf V et al (1997) Ligand-dependent development of the endothelial and hemopoietic lineages from embryonic mesodermal cells expressing vascular endothelial growth factor receptor 2. *Proc Natl Acad Sci* 94:5141–5146. <https://doi.org/10.1073/pnas.94.10.5141>
 32. Fang S, Nurmi H, Heinolainen K et al (2016) Critical requirement of VEGF-C in transition to fetal erythropoiesis. *Blood* 128:710–720. <https://doi.org/10.1182/blood-2015-12-687970>
 33. Fang S, Chen S, Nurmi H et al (2020) VEGF-C protects the integrity of the bone marrow perivascular niche in mice. *Blood* 136:1871–1883. <https://doi.org/10.1182/blood.2020005699>
 34. Thiele W, Krishnan J, Rothley M et al (2012) VEGFR-3 is expressed on megakaryocyte precursors in the murine bone marrow and plays a regulatory role in megakaryopoiesis. *Blood* 120:1899–1907. <https://doi.org/10.1182/blood-2011-09-376657>
 35. Heino TI, Kärpänen T, Wahlström G et al (2001) The *Drosophila* VEGF receptor homolog is expressed in hemocytes. *Mech Dev* 109:69–77. [https://doi.org/10.1016/S0925-4773\(01\)00510-X](https://doi.org/10.1016/S0925-4773(01)00510-X)
 36. Read RD (2018) Pvr receptor tyrosine kinase signaling promotes post-embryonic morphogenesis, and survival of glia and neural progenitor cells in *Drosophila*. *Development*. <https://doi.org/10.1242/dev.164285>
 37. Zheng H, Wang X, Guo P et al (2017) Premature remodeling of fat body and fat mobilization triggered by platelet-derived growth factor/VEGF receptor in *Drosophila*. *FASEB J* 31:1964–1975. <https://doi.org/10.1096/fj.201601127R>
 38. Tarsitano M, Falco SD, Colonna V et al (2006) The *C. elegans* pvf-1 gene encodes a PDGF/VEGF-like factor able to bind mammalian VEGF receptors and to induce angiogenesis. *FASEB J* 20:227–233. <https://doi.org/10.1096/fj.05-4147com>
 39. Dalpe G, Tarsitano M, Persico MG et al (2013) *C. elegans* PVF-1 inhibits permissive UNC-40 signalling through CED-10 GTPase to position the male ray 1 sensillum. *Development* 140:4020–4030. <https://doi.org/10.1242/dev.095190>
 40. Dormer A, Beck G (2005) Evolutionary analysis of human vascular endothelial growth factor, angiopoietin, and tyrosine endothelial kinase involved in angiogenesis and immunity. *In Silico Biol* 5:323–339. https://doi.org/10.1007/978-3-540-33177-3_23
 41. Holmes DI, Zachary I (2005) The vascular endothelial growth factor (VEGF) family: angiogenic factors in health and disease. *Genome Biol* 6:209. <https://doi.org/10.1186/gb-2005-6-2-209>
 42. Kasap M (2005) Phylogenetic analysis of vascular endothelial growth factor diversity. *Turk J Biol* 29:217–227
 43. He W, Tang Y, Qi B et al (2014) Phylogenetic analysis and positive-selection site detecting of vascular endothelial growth factor family in vertebrates. *Gene* 535:345–352. <https://doi.org/10.1016/j.gene.2013.10.031>
 44. Hinchliff CE, Smith SA, Allman JF et al (2015) Synthesis of phylogeny and taxonomy into a comprehensive tree of life. *Proc Natl Acad Sci* 112:12764–12769. <https://doi.org/10.1073/pnas.1423041112>
 45. Krishnapati L-S, Ghaskadbi S (2014) Identification and characterization of VEGF and FGF from Hydra. *Int J Dev Biol* 57:897–906. <https://doi.org/10.1387/ijdb.130077sg>
 46. Seipel K, Eberhardt M, Müller P et al (2004) Homologs of vascular endothelial growth factor and receptor, VEGF and VEGFR, in the jellyfish *Podocoryne carnea*. *Dev Dyn* 231:303–312. <https://doi.org/10.1002/dvdy.20139>
 47. Turwankar A, Ghaskadbi S (2019) VEGF and FGF signaling during head regeneration in hydra. *bioRxiv*. <https://doi.org/10.1101/596734>
 48. Dehal P, Boore JL (2005) Two rounds of whole genome duplication in the ancestral vertebrate. *PLOS Biol* 3:e314. <https://doi.org/10.1371/journal.pbio.0030314>
 49. Kasahara M (2007) The 2R hypothesis: an update. *Curr Opin Immunol* 19:547–552. <https://doi.org/10.1016/j.coi.2007.07.009>
 50. Hughes LC, Ortí G, Huang Y et al (2018) Comprehensive phylogeny of ray-finned fishes (Actinopterygii) based on transcriptomic and genomic data. *Proc Natl Acad Sci* 115:6249–6254. <https://doi.org/10.1073/pnas.1719358115>
 51. Das RN, Tevet Y, Safriel S et al (2022) Generation of specialized blood vessels via lymphatic transdifferentiation. *Nature* 606:570–575. <https://doi.org/10.1038/s41586-022-04766-2>
 52. Pasquier J, Cabau C, Nguyen T et al (2016) Gene evolution and gene expression after whole genome duplication in fish: the PhyloFish database. *BMC Genomics* 17:368. <https://doi.org/10.1186/s12864-016-2709-z>
 53. Berthelot C, Brunet F, Chalopin D et al (2014) The rainbow trout genome provides novel insights into evolution after whole-genome duplication in vertebrates. *Nat Commun* 5:3657. <https://doi.org/10.1038/ncomms4657>

54. Macqueen DJ, Johnston IA (2014) A well-constrained estimate for the timing of the salmonid whole genome duplication reveals major decoupling from species diversification. *Proc R Soc B Biol Sci*. <https://doi.org/10.1098/rspb.2013.2881>
55. Postlethwait JH, Woods IG, Ngo-Hazelett P et al (2000) Zebrafish comparative genomics and the origins of vertebrate chromosomes. *Genome Res* 10:1890–1902. <https://doi.org/10.1101/gr.164800>
56. Lynch M, Force A (2000) The probability of duplicate gene preservation by subfunctionalization. *Genetics* 154:459–473. <https://doi.org/10.1093/genetics/154.1.459>
57. Cunningham F, Achuthan P, Akanni W et al (2019) Ensembl 2019. *Nucleic Acids Res* 47:D745–D751. <https://doi.org/10.1093/nar/gky1113>
58. Chang ES, Neuhof M, Rubinstein ND et al (2015) Genomic insights into the evolutionary origin of Myxozoa within Cnidaria. *Proc Natl Acad Sci* 112:14912–14917. <https://doi.org/10.1073/pnas.1511468112>
59. Ramachandran RK, Govindarajan V, Seid CA et al (1995) Role for platelet-derived growth factor-like and epidermal growth factor-like signaling pathways in gastrulation and spiculogenesis in the *Lytechinus* sea urchin embryo. *Dev Dyn Off Publ Am Assoc Anat* 204:77–88. <https://doi.org/10.1002/aja.1002040110>
60. Heimberg AM, Cowper-Sallari R, Sémon M et al (2010) microRNAs reveal the interrelationships of hagfish, lampreys, and gnathostomes and the nature of the ancestral vertebrate. *Proc Natl Acad Sci* 107:19379–19383. <https://doi.org/10.1073/pnas.1010350107>
61. Janvier P (2010) microRNAs revive old views about jawless vertebrate divergence and evolution. *Proc Natl Acad Sci* 107:19137–19138. <https://doi.org/10.1073/pnas.1014583107>
62. Huemer HP, Zobl A, Windisch A (2014) Serological evidence for Parapoxvirus infection in chamois from the Tyrol regions of Austria and Italy. *Vet Ital*. <https://doi.org/10.12834/VetIt.1304.14>
63. Baldwin ME, Halford MM, Roufail S et al (2005) Vascular endothelial growth factor D is dispensable for development of the lymphatic system. *Mol Cell Biol* 25:2441–2449. <https://doi.org/10.1128/MCB.25.6.2441-2449.2005>
64. Leppänen V-M, Prota AE, Jeltsch M et al (2010) Structural determinants of growth factor binding and specificity by VEGF receptor 2. *Proc Natl Acad Sci* 107:2425–2430. <https://doi.org/10.1073/pnas.0914318107>
65. Leppänen V-M, Jeltsch M, Anisimov A et al (2011) Structural determinants of vascular endothelial growth factor-D receptor binding and specificity. *Blood* 117:1507–1515. <https://doi.org/10.1182/blood-2010-08-301549>
66. Wiesmann C, Fuh G, Christinger HW et al (1997) Crystal structure at 1.7 Å resolution of VEGF in complex with domain 2 of the Flt-1 receptor. *Cell* 91:695–704. [https://doi.org/10.1016/S0092-8674\(00\)80456-0](https://doi.org/10.1016/S0092-8674(00)80456-0)
67. Künnapu J, Bokharai H, Jeltsch M (2021) Proteolytic cleavages in the VEGF family: generating diversity among angiogenic VEGFs, essential for the activation of lymphangiogenic VEGFs. *Biology* 10:167. <https://doi.org/10.3390/biology10020167>
68. Rodi DJ, Mandava S, Makowski L (2004) DIVAA: analysis of amino acid diversity in multiple aligned protein sequences. *Bioinformatics* 20:3481–3489. <https://doi.org/10.1093/bioinformatics/bth432>
69. Bates DO, Cui T-G, Doughty JM et al (2002) VEGF165b, an inhibitory splice variant of vascular endothelial growth factor, is down-regulated in renal cell carcinoma. *Cancer Res* 62:4123–4131
70. Eswarappa SM, Potdar AA, Koch WJ et al (2014) Programmed translational read-through generates anti-angiogenic VEGF-Ax. *Cell* 157:1605–1618. <https://doi.org/10.1016/j.cell.2014.04.033>
71. Sibley CR, Blazquez L, Ule J (2016) Lessons from non-canonical splicing. *Nat Rev Genet* 17:407–421. <https://doi.org/10.1038/nrg.2016.46>
72. Mi H, Muruganujan A, Thomas PD (2013) PANTHER in 2013: modeling the evolution of gene function, and other gene attributes, in the context of phylogenetic trees. *Nucleic Acids Res* 41:D377–386. <https://doi.org/10.1093/nar/gks1118>
73. Lee MSY, Soubrier J, Edgecombe GD (2013) Rates of phenotypic and genomic evolution during the Cambrian explosion. *Curr Biol* 23:1889–1895. <https://doi.org/10.1016/j.cub.2013.07.055>
74. Erwin DH, Davidson EH (2002) The last common bilaterian ancestor. *Development* 129:3021–3032. <https://doi.org/10.1242/dev.129.13.3021>
75. Hickman CP, Roberts LS, Keen SL et al (2008) Annelids and allied Taxa, Clade Clitellata. *Integrated principles of zoology*, 14th edn. McGraw-Hill/Higher Education, Boston, pp 371–375
76. Monahan-Earley R, Dvorak AM, Aird WC (2013) Evolutionary origins of the blood vascular system and endothelium. *J Thromb Haemost JTH* 11:46–66. <https://doi.org/10.1111/jth.12253>
77. Barber VC, Graziadei P (1965) The fine structure of cephalopod blood vessels. I. Some smaller peripheral vessels. *Z Zellforsch Mikrosk Anat Vienna Austria* 66:765–781. <https://doi.org/10.1007/BF00342955>
78. de Eguileor M, Grimaldi A, Tettamanti G et al (2001) Ultrastructure and functional versatility of hirudinean botryoidal tissue. *Tissue Cell* 33:332–341. <https://doi.org/10.1054/tice.2001.0181>
79. Styfhals R, Zolotarov G, Hulselmans G et al (2022) Cell type diversity in a developing octopus brain. *Nat Commun* 13:7392. <https://doi.org/10.1038/s41467-022-35198-1>
80. Tettamanti G, Grimaldi A, Valvassori R et al (2003) Vascular endothelial growth factor is involved in neoangiogenesis in *Hirudo medicinalis* (Annelida, Hirudinea). *Cytokine* 22:168–179. [https://doi.org/10.1016/S1043-4666\(03\)00176-5](https://doi.org/10.1016/S1043-4666(03)00176-5)
81. Cao N, Yao Z-X (2011) The hemangioblast: from concept to authentication. *Anat Rec* 294:580–588. <https://doi.org/10.1002/ar.21360>
82. Moorman AFM, Christoffels VM (2003) Cardiac chamber formation: development, genes, and evolution. *Physiol Rev* 83:1223–1267. <https://doi.org/10.1152/physrev.00006.2003>
83. Hellstrom M, Kalén M, Lindahl P et al (1999) Role of PDGF-B and PDGFR-beta in recruitment of vascular smooth muscle cells and pericytes during embryonic blood vessel formation in the mouse. *Development* 126:3047–3055. <https://doi.org/10.1242/dev.126.14.3047>
84. Tiozzo S, Voskoboinik A, Brown FD, De Tomaso AW (2008) A conserved role of the VEGF pathway in angiogenesis of an ectodermally-derived vasculature. *Dev Biol* 315:243–255. <https://doi.org/10.1016/j.ydbio.2007.12.035>
85. Olofsson B, Pajusola K, Kaipainen A et al (1996) Vascular endothelial growth factor B, a novel growth factor for endothelial cells. *Proc Natl Acad Sci* 93:2576–2581. <https://doi.org/10.1073/pnas.93.6.2576>
86. Hargreaves AD, Swain MT, Logan DW, Mulley JF (2014) Testing the Toxicofera: comparative transcriptomics casts doubt on the single, early evolution of the reptile venom system. *Toxicon* 92:140–156. <https://doi.org/10.1016/j.toxicon.2014.10.004>
87. Nakatani Y, Shingate P, Ravi V et al (2021) Reconstruction of proto-vertebrate, proto-cyclostome and proto-gnathostome genomes provides new insights into early vertebrate evolution. *Nat Commun* 12:4489. <https://doi.org/10.1038/s41467-021-24573-z>

88. Alkharsah KR (2018) VEGF upregulation in viral infections and its possible therapeutic implications. *Int J Mol Sci* 19:1642. <https://doi.org/10.3390/ijms19061642>
89. Inder MK, Ueda N, Mercer AA et al (2007) Bovine papular stomatitis virus encodes a functionally distinct VEGF that binds both VEGFR-1 and VEGFR-2. *J Gen Virol* 88:781–791. <https://doi.org/10.1099/vir.0.82582-0>
90. Lyttle DJ, Fraser KM, Fleming SB et al (1994) Homologs of vascular endothelial growth factor are encoded by the poxvirus orf virus. *J Virol* 68:84–92. <https://doi.org/10.1128/JVI.68.1.84-92.1994>
91. Ueda N, Wise LM, Stacker SA et al (2003) Pseudocowpox virus encodes a homolog of vascular endothelial growth factor. *Virology* 305:298–309. <https://doi.org/10.1006/viro.2002.1750>
92. Savory LJ, Stacker SA, Fleming SB et al (2000) Viral vascular endothelial growth factor plays a critical role in Orf virus infection. *J Virol* 74:10699–10706. <https://doi.org/10.1128/JVI.74.22.10699-10706.2000>
93. de Groof A, Guelen L, Deijs M et al (2015) A novel virus causes scale drop disease in *Lates calcarifer*. *PLOS Pathog* 11:e1005074. <https://doi.org/10.1371/journal.ppat.1005074>
94. Essbauer S, Pfeffer M, Meyer H (2010) Zoonotic poxviruses. *Vet Microbiol* 140:229–236. <https://doi.org/10.1016/j.vetmic.2009.08.026>
95. Hautaniemi M, Ueda N, Tuimala J et al (2010) The genome of pseudocowpoxvirus: comparison of a reindeer isolate and a reference strain. *J Gen Virol* 91:1560–1576. <https://doi.org/10.1099/vir.0.018374-0>
96. Whittington RJ, Becker JA, Dennis MM (2010) Iridovirus infections in finfish—critical review with emphasis on ranaviruses. *J Fish Dis* 33:95–122. <https://doi.org/10.1111/j.1365-2761.2009.01110.x>
97. Jha SK, Rauniyar K, Karpanen T et al (2017) Efficient activation of the lymphangiogenic growth factor VEGF-C requires the C-terminal domain of VEGF-C and the N-terminal domain of CCBE1. *Sci Rep* 7:4916. <https://doi.org/10.1038/s41598-017-04982-1>
98. Lackner M, Schmotz C, Jeltsch M (2019) The proteolytic activation of vascular endothelial growth factor-C. *Lymphol Forsch Prax* 23:88–98. <https://doi.org/10.5281/zenodo.3629263>
99. Plouët J, Moro F, Bertagnonli S et al (1997) Extracellular cleavage of the vascular endothelial growth factor 189-amino acid form by urokinase is required for its mitogenic effect. *J Biol Chem* 272:13390–13396. <https://doi.org/10.1074/jbc.272.20.13390>
100. Park JE, Keller GA, Ferrara N (1993) The vascular endothelial growth factor (VEGF) isoforms: differential deposition into the subepithelial extracellular matrix and bioactivity of extracellular matrix-bound VEGF. *Mol Biol Cell* 4:1317–1326
101. Chen TT, Luque A, Lee S et al (2010) Anchorage of VEGF to the extracellular matrix conveys differential signaling responses to endothelial cells. *J Cell Biol* 188:595–609. <https://doi.org/10.1083/jcb.200906044>
102. Lee S, Jilani SM, Nikolova GV et al (2005) Processing of VEGF-A by matrix metalloproteinases regulates bioavailability and vascular patterning in tumors. *J Cell Biol* 169:681–691. <https://doi.org/10.1083/jcb.200409115>
103. Ruhrberg C, Gerhardt H, Golding M et al (2002) Spatially restricted patterning cues provided by heparin-binding VEGF-A control blood vessel branching morphogenesis. *Genes Dev* 16:2684–2698. <https://doi.org/10.1101/gad.242002>
104. Gerhardt H, Golding M, Fruttiger M et al (2003) VEGF guides angiogenic sprouting utilizing endothelial tip cell filopodia. *J Cell Biol* 161:1163–1177. <https://doi.org/10.1083/jcb.200302047>
105. Lundkvist A, Lee S, Iruela-Arispe L et al (2007) Growth factor gradients in vascular patterning. In: Chadwick DJ, Goode J (eds) *Vascular development*. John Wiley & Sons Ltd, pp 194–206
106. Carmeliet P, Ng Y-S, Nuyens D et al (1999) Impaired myocardial angiogenesis and ischemic cardiomyopathy in mice lacking the vascular endothelial growth factor isoforms VEGF 164 and VEGF 188. *Nat Med* 5:495–502. <https://doi.org/10.1038/8379>
107. Stalmans I, Ng Y-S, Rohan R et al (2002) Arteriolar and venular patterning in retinas of mice selectively expressing VEGF isoforms. *J Clin Invest* 109:327–336. <https://doi.org/10.1172/JCI14362>
108. Robinson CJ, Stringer SE (2001) The splice variants of vascular endothelial growth factor (VEGF) and their receptors. *J Cell Sci* 114:853–865
109. Bahary N, Goishi K, Stuckenholtz C et al (2007) Duplicate VegfA genes and orthologues of the KDR receptor tyrosine kinase family mediate vascular development in the zebrafish. *Blood* 110:3627–3636. <https://doi.org/10.1182/blood-2006-04-016378>
110. Kikuchi R, Nakamura K, MacLauchlan S et al (2014) An anti-angiogenic isoform of VEGF-A contributes to impaired vascularization in peripheral artery disease. *Nat Med* 20:1464–1471. <https://doi.org/10.1038/nm.3703>
111. Xin H, Zhong C, Nudleman E, Ferrara N (2016) Evidence for pro-angiogenic functions of VEGF-Ax. *Cell* 167:275–284.e6. <https://doi.org/10.1016/j.cell.2016.08.054>
112. Soker S, Takashima S, Miao HQ et al (1998) Neuropilin-1 is expressed by endothelial and tumor cells as an isoform-specific receptor for vascular endothelial growth factor. *Cell* 92:735–745. [https://doi.org/10.1016/S0092-8674\(00\)81402-6](https://doi.org/10.1016/S0092-8674(00)81402-6)
113. Parker MW, Xu P, Li X, Vander Kooi CW (2012) Structural basis for selective vascular endothelial growth factor-A (VEGF-A) binding to neuropilin-1. *J Biol Chem* 287:11082–11089. <https://doi.org/10.1074/jbc.M111.331140>
114. Balistreri G, Yamauchi Y, Teesalu T (2021) A widespread viral entry mechanism: the C-end Rule motif–neuropilin receptor interaction. *Proc Natl Acad Sci* 118:e2112457118. <https://doi.org/10.1073/pnas.2112457118>
115. Peach CJ, Mignone VW, Arruda MA et al (2018) Molecular pharmacology of VEGF-A isoforms: binding and signalling at VEGFR2. *Int J Mol Sci* 19:1264. <https://doi.org/10.3390/ijms19041264>
116. Gu W, Li M, Xu Y et al (2014) The impact of RNA structure on coding sequence evolution in both bacteria and eukaryotes. *BMC Evol Biol* 14:87. <https://doi.org/10.1186/1471-2148-14-87>
117. Dardente H, English WR, Valluru MK et al (2020) Debunking the myth of the endogenous antiangiogenic Vegfxxx b transcripts. *Trends Endocrinol Metab* 31:398–409. <https://doi.org/10.1016/j.tem.2020.01.014>
118. Harris S, Craze M, Newton J et al (2012) Do anti-angiogenic VEGF (VEGFxxx b) isoforms exist? A cautionary tale. *PLoS ONE*. <https://doi.org/10.1371/journal.pone.0035231>
119. Bourque G, Burns KH, Gehring M et al (2018) Ten things you should know about transposable elements. *Genome Biol* 19:199. <https://doi.org/10.1186/s13059-018-1577-z>
120. Lynch VJ, Leclerc RD, May G, Wagner GP (2011) Transposon-mediated rewiring of gene regulatory networks contributed to the evolution of pregnancy in mammals. *Nat Genet* 43:1154–1159. <https://doi.org/10.1038/ng.917>
121. Chen HI, Poduri A, Numi H et al (2014) VEGF-C and aortic cardiomyocytes guide coronary artery stem development. *J Clin Invest* 124:4899–4914. <https://doi.org/10.1172/JCI77483>
122. Dumont DJ, Jussila L, Taipale J et al (1998) Cardiovascular failure in mouse embryos deficient in VEGF receptor-3. *Science* 282:946–949. <https://doi.org/10.1126/science.282.5390.946>

123. Iyer S, Acharya KR (2011) Tying the knot: the cystine signature and molecular-recognition processes of the vascular endothelial growth factor family of angiogenic cytokines. *FEBS J* 278:4304–4322. <https://doi.org/10.1111/j.1742-4658.2011.08350.x>
124. Rauniyar K, Akhondzadeh S, Gaciarz A et al (2022) Bioactive VEGF-C from *E. coli*. *Sci Rep* 12:18157. <https://doi.org/10.1038/s41598-022-22960-0>
125. Narayan M (2020) Revisiting the formation of a native disulfide bond: consequences for protein regeneration and beyond. *Molecules* 25:5337. <https://doi.org/10.3390/molecules25225337>
126. Muller YA, Heiring C, Misselwitz R et al (2002) The cystine knot promotes folding and not thermodynamic stability in vascular endothelial growth factor. *J Biol Chem* 277:43410–43416. <https://doi.org/10.1074/jbc.M206438200>
127. Hagberg C, Mehlem A, Falkevall A et al (2013) Endothelial fatty acid transport: role of vascular endothelial growth factor B. *Physiology* 28:125–134. <https://doi.org/10.1152/physiol.00042.2012>
128. Anisimov A, Leppanen V-M, Tvorogov D et al (2013) The basis for the distinct biological activities of vascular endothelial growth factor receptor-1 ligands. *Sci Signal*. <https://doi.org/10.1126/scisignal.2003905>
129. Moessinger C, Nilsson I, Muhl L et al (2020) VEGF-B signaling impairs endothelial glucose transcytosis by decreasing membrane cholesterol content. *EMBO Rep* 21:e49343. <https://doi.org/10.15252/embr.201949343>
130. Zafar MI, Zheng J, Kong W et al (2017) The role of vascular endothelial growth factor-B in metabolic homeostasis: current evidence. *Biosci Rep* 37:BSR20171089. <https://doi.org/10.1042/BSR20171089>
131. Butler PJ (2016) The physiological basis of bird flight. *Philos Trans R Soc B Biol Sci* 371:20150384. <https://doi.org/10.1098/rstb.2015.0384>
132. Woodhouse M, Burkart-Waco D, Comai L (2009) Polyploidy. *Nat Educ* 2:1
133. Jha SK, Rauniyar K, Chronowska E et al (2019) KLK3/PSA and cathepsin D activate VEGF-C and VEGF-D. *Elife* 8:e44478. <https://doi.org/10.7554/eLife.44478>
134. Krabbenhoft TJ, MacGuigan DJ, Backenstose NJC et al (2021) Chromosome-level genome assembly of chinese sucker (*Myxocyprinus asiaticus*) reveals strongly conserved synteny following a catostomid-specific whole-genome duplication. *Genome Biol Evol* 13:evab190. <https://doi.org/10.1093/gbe/evab190>
135. Uyeno T, Smith GR (1972) Tetraploid origin of the karyotype of catostomid fishes. *Science* 175:644–646. <https://doi.org/10.1126/science.175.4022.644>
136. Larhammar D, Risinger C (1994) Molecular genetic aspects of tetraploidy in the common carp *Cyprinus carpio*. *Mol Phylogenet Evol* 3:59–68. <https://doi.org/10.1006/mpev.1994.1007>
137. Xu P, Xu J, Liu G et al (2019) The allotetraploid origin and asymmetrical genome evolution of the common carp *Cyprinus carpio*. *Nat Commun* 10:4625. <https://doi.org/10.1038/s41467-019-12644-1>
138. Christoffels A, Koh EGL, Chia J et al (2004) Fugu genome analysis provides evidence for a whole-genome duplication early during the evolution of ray-finned fishes. *Mol Biol Evol* 21:1146–1151. <https://doi.org/10.1093/molbev/msh114>
139. Rouchka E, Cha I (2009) Current trends in pseudogene detection and characterization. *Curr Bioinforma* 4:112–119. <https://doi.org/10.2174/157489309788184792>
140. Lange M, Ohnesorge N, Hoffmann D et al (2022) Zebrafish mutants in vegfab can affect endothelial cell proliferation without altering ERK phosphorylation and are phenocopied by loss of PI3K signaling. *Dev Biol* 486:26–43. <https://doi.org/10.1016/j.ydbio.2022.03.006>
141. Weijts BGMW, Bakker WJ, Cornelissen PWA et al (2012) E2F7 and E2F8 promote angiogenesis through transcriptional activation of VEGFA in cooperation with HIF1. *EMBO J* 31:3871–3884. <https://doi.org/10.1038/emboj.2012.231>
142. Bower NI, Vogrin AJ, Guen LL et al (2017) Vegfd modulates both angiogenesis and lymphangiogenesis during zebrafish embryonic development. *Development* 144:507–518. <https://doi.org/10.1242/dev.146969>
143. Vogrin AJ, Bower NI, Gunzburg MJ et al (2019) Evolutionary differences in the Vegf/Vegfr code reveal organotypic roles for the endothelial cell receptor Kdr in developmental lymphangiogenesis. *Cell Rep* 28:2023–2036.e4. <https://doi.org/10.1016/j.celrep.2019.07.055>
144. Tzahor E, Yaniv K (2022) How many fish make a mouse? *Nat Cardiovasc Res* 1:2–3. <https://doi.org/10.1038/s44161-021-00010-8>
145. Jeltsch M, Alitalo K (2022) Lymphatic-to-blood vessel transdifferentiation in zebrafish. *Nat Cardiovasc Res* 1:539–541. <https://doi.org/10.1038/s44161-022-00073-1>
146. Guindon S, Dufayard J-F, Lefort V et al (2010) New algorithms and methods to estimate maximum-likelihood phylogenies: assessing the performance of PhyML 3.0. *Syst Biol* 59:307–321. <https://doi.org/10.1093/sysbio/syq010>
147. Pond SLK, Frost SDW, Muse SV (2005) HyPhy: hypothesis testing using phylogenies. *Bioinformatics* 21:676–679. <https://doi.org/10.1093/bioinformatics/bti079>
148. Letunic I, Bork P (2021) Interactive tree of life (iTOL) v5: an online tool for phylogenetic tree display and annotation. *Nucleic Acids Res* 49:W293–W296. <https://doi.org/10.1093/nar/gkab301>
149. Notredame C, Higgins DG, Heringa J (2000) T-coffee: a novel method for fast and accurate multiple sequence alignment 1 | Edited by J Thornton. *J Mol Biol* 302:205–217. <https://doi.org/10.1006/jmbi.2000.4042>
150. Wallace IM, O'Sullivan O, Higgins DG, Notredame C (2006) M-Coffee: combining multiple sequence alignment methods with T-Coffee. *Nucleic Acids Res* 34:1692–1699. <https://doi.org/10.1093/nar/gkl091>
151. Suyama M, Torrents D, Bork P (2006) PAL2NAL: robust conversion of protein sequence alignments into the corresponding codon alignments. *Nucleic Acids Res* 34:W609–612. <https://doi.org/10.1093/nar/gkl315>
152. Kosakovsky Pond SL, Frost SDW (2005) Not so different after all: a comparison of methods for detecting amino acid sites under selection. *Mol Biol Evol* 22:1208–1222. <https://doi.org/10.1093/molbev/msi105>
153. Sayers EW, Bolton EE, Brister JR et al (2022) Database resources of the national center for biotechnology information. *Nucleic Acids Res* 50:D20–D26. <https://doi.org/10.1093/nar/gkab1112>
154. Castresana J (2000) Selection of conserved blocks from multiple alignments for their use in phylogenetic analysis. *Mol Biol Evol* 17:540–552. <https://doi.org/10.1093/oxfordjournals.molbev.a026334>

Publisher's Note Springer Nature remains neutral with regard to jurisdictional claims in published maps and institutional affiliations.